

The interstellar medium conditions of a strong Ly α emitter at $z = 8.279$ revealed by JWST: a robust LyC leaker candidate at the Epoch of Reionization

RAFAEL NAVARRO-CARRERA,¹ KARINA I. CAPUTI,^{1,2} EDOARDO IANI,¹ PIERLUIGI RINALDI,^{3,1} VASILY KOKOREV,⁴ AND JOSEPHINE KERUTT¹

¹*Kapteyn Astronomical Institute, University of Groningen, P.O. Box 800, 9700AV Groningen, The Netherlands*

²*Cosmic Dawn Center (DAWN), Copenhagen, Denmark*

³*Steward Observatory, University of Arizona, 933 North Cherry Avenue, Tucson, AZ 85721, USA*

⁴*Department of Astronomy, The University of Texas at Austin, Austin, TX 78712, USA*

Submitted to ApJ

ABSTRACT

Making use of JWST NIRSpec and NIRCам data, we conduct a detailed analysis of GN- $z8$ -LAE, a strong Ly α emitter at $z = 8.279$. We investigate the interstellar medium (ISM) conditions that enable the Ly α detection in this source at the Epoch of Reionization (EoR), and scrutinize GN- $z8$ -LAEs as an early reionizer. In agreement with previous results, we find that GN- $z8$ -LAE is a young galaxy (age ~ 10 Myr) with lower stellar mass ($M^* \sim 10^{7.66} M_\odot$) than most Ly α emitters at similar redshifts. The derived stellar mass and star formation rate surface densities are $\Sigma_{M^*} \sim 355 M_\odot/\text{pc}^2$ and $\Sigma_{\text{SFR}} \sim 88 M_\odot \text{ yr}^{-1} \text{ kpc}^2$, respectively. Our spectral analysis indicates that: the Ly α line peak has a small velocity offset $\Delta v = 133 \pm 72 \text{ km/s}$ with respect to the galaxy systemic redshift; $\text{CIV]/CIII]} \approx 3.3$; the ISM is characterized by a hard ionization field, although no signature of AGN is present. Moreover, we report the presence of NIII] $\lambda 1750$ emission implying super-solar N abundance, which makes GN- $z8$ -LAE one of the first strong Ly α and nitrogen emitters at the EoR. Based on all these properties, we apply a wide range of methods to constrain the Lyman continuum escape fraction ($f_{\text{esc}}^{\text{LyC}}$) of GN- $z8$ -LAE and report $f_{\text{esc}}^{\text{LyC}} > 14\%$ in all cases. Therefore, we conclude that GN- $z8$ -LAE is a robust candidate for a Lyman continuum (LyC) leaker at the EoR which is being caught at the moment of efficiently reionizing its surrounding medium.

Keywords: High-redshift galaxies (734) – James Webb Space Telescope (2291) – Galaxy evolution (594) – Infrared astronomy (786) – Galaxy photometry (611) – Infrared spectroscopy (2285) – LAE (978)

1. INTRODUCTION

Finding the sources that reionized the Universe within the first billion years of cosmic time constitutes one of the main goals of extragalactic astronomy. Based on a number of observational constraints, it has been determined that the Epoch of Reionization (EoR) occurred between redshifts $z \approx 10$ and $z \approx 6$ (Robertson et al. 2015), although some recent quasar studies suggest that

it would have only been completed by redshift $z \approx 5.3$ (Kulkarni et al. 2019; Bosman et al. 2022).

During this period, the intergalactic medium changed progressively from a state dominated by neutral atomic hydrogen (HI) to a phase with virtually all atomic H ionized. This process requires that sufficient H ionizing photons (with energy $\geq 13.6 \text{ eV}$) are produced within galaxies and can escape their interstellar media to reach and ionize their circumgalactic gas. Reionization is, therefore, depicted as a process in which growing bubbles of ionized gas progressively fill the intergalactic medium until making it completely transparent (e.g., Dayal & Ferrara 2018).

The opacity of the IGM during the EoR prevents direct observation of basically all the H-ionizing photons produced by galaxies at that time. Indeed, there is a declining incidence of Ly α emitting galaxies at $z \gtrsim 6$ (e.g., Stark et al. 2010; Fontana et al. 2010; Pentericci et al. 2011; Caruana et al. 2014; Schenker et al. 2014). However, this decline is less evident in the most luminous star-forming galaxies, with several examples of bright Ly α emitters found at $z \sim 7-8$ (e.g., Zitrin et al. 2015; Roberts-Borsani et al. 2016; Stark et al. 2017; Kumari et al. 2024; Witstok et al. 2024a). These sources constitute an excellent laboratory to investigate how the patchy reionization process evolved in the first billion years of cosmic time.

An alternative approach to understanding the drivers of reionization is to study the so-called Lyman continuum (LyC) leakers at low and intermediate redshifts (e.g., Leitherer et al. 1995; Steidel et al. 2001; Vanzella et al. 2018; Flury et al. 2022). These are rare star-forming galaxies in which a significant amount of ionizing photons are able to escape the source and its circumgalactic medium (CGM) to reach the observer. If the escape fraction is $f_{\text{esc}} \gtrsim 0.1$, then the LyC leaker is considered a good analog of the sources of reionization. This is because it is estimated that star-forming galaxies at high z must have had $f_{\text{esc}} \gtrsim 0.1$ to have efficiently conducted the reionization process (e.g., Rosdahl et al. 2018), although some observational studies concluded that a value $\gtrsim 0.05$ could be enough (Atek et al. 2024).

As the LyC leakage cannot be directly observed at the EoR, considerable effort has been devoted to identifying other photometric and spectroscopic properties that characterize LyC leakers. These galaxies typically show compact morphologies with high star formation rate densities (Σ_{SFR} ; e.g., Naidu et al. 2020); a steep UV continuum; a narrow Ly α line with high rest-frame EW ($> 70 \text{ \AA}$) and with a small velocity offset ($< 200 \text{ km/s}$) with respect to the galaxy systemic redshift derived from other emission lines (Verhamme et al. 2017; Izotov et al. 2018); a line ratio $[\text{OIII}]\lambda 4959, 5007 / [\text{OII}]\lambda 3727, 3729 \gtrsim 5$ (Nakajima & Ouchi 2014; Izotov et al. 2017; Flury et al. 2022); and strong CIV emission, with $\text{C IV}\lambda 1550 / \text{C III}\lambda 1909 \gtrsim 0.75$ (Schaerer et al. 2022), among others. However, very rarely have all these properties been reported together in LyC leakers.

With its high sensitivity up to mid-infrared wavelengths, JWST (Gardner et al. 2023) is making the study of galaxies within the EoR routinely possible (e.g., Endsley et al. 2023; Rinaldi et al. 2023, 2024a; Caputi et al. 2024; Iani et al. 2024a; Bunker et al. 2023; Donnan et al. 2023; Castellano et al. 2024; Harikane et al.

2024). JWST spectroscopic capabilities in the infrared allow for unprecedented investigations of the interstellar media in some of these sources (e.g., Bunker et al. 2023; Matthee et al. 2023; Schaerer et al. 2024). These studies point towards the presence of relatively extreme interstellar medium conditions, which are not typically found at lower redshifts (e.g., Meštrić et al. 2022; Vanzella et al. 2023). With JWST spectroscopy one can search, in particular, for the signatures that characterize LyC leakers (e.g., Mascia et al. 2023a). Moreover, JWST spectra have enabled the discovery of unexpected emission lines whose origin is difficult to explain, such as $\text{NeIII}]\lambda 1749 - 1753$ and $\text{NIV}]\lambda 1486$, which has recently been reported in a number of high- z objects (e.g., Isobe et al. 2023; Marques-Chaves et al. 2024; Schaerer et al. 2024).

In this work, we present a detailed spectroscopic and photometric study of GN-z8-LAE, a strong Ly α emitter at $z = 8.279$ selected from the public JWST Advanced Deep Extragalactic Survey (JADES; Eisenstein et al. 2023a) in GOODS-North. This source was previously studied in other works (e.g., Hainline et al. 2024) and within a sample of high- z Ly α emitters by Witstok et al. (2024a) (under the name JADES-GN-z8-0-LA) who inferred that it could have a very high escape fraction and lived in a large ionized bubble, with the likely presence of interacting companions. Here we perform an independent study of the JWST data for this source, particularly extending the analysis of spectral properties in order to obtain a more complete understanding of the physical conditions of this strong early reionizer candidate.

Our paper is structured as follows. In Section 2 we describe the datasets used in our study. We present our independent derivation of the main physical properties of GN-z8-LAE, based on the analysis of both spectroscopic and photometric data, in Section 3. In Section 4 we test all the main criteria to identify LyC leakers and show that GN-z8-LAE complies with all of them. Finally, in Section 5 we summarize our findings and present some concluding remarks. We adopt throughout a flat Λ CDM cosmology with $\Omega_{\text{M}} = 0.3$, $\Omega_{\Lambda} = 0.7$ and $H_0 = 70 \text{ km s}^{-1} \text{ Mpc}^{-1}$, and a Kroupa initial mass function (Kroupa 2001). In all cases, the term ‘escape fraction’ (f_{esc}) refers to its absolute value.

2. DATA

We use the publicly available spectroscopic and photometric data from JADES (Eisenstein et al. 2023b) in the GOODS-N, as part of the Public Data Release 3 (D’Eugenio et al. 2024). It contains several thousands of readily available reduced, extracted, and cal-

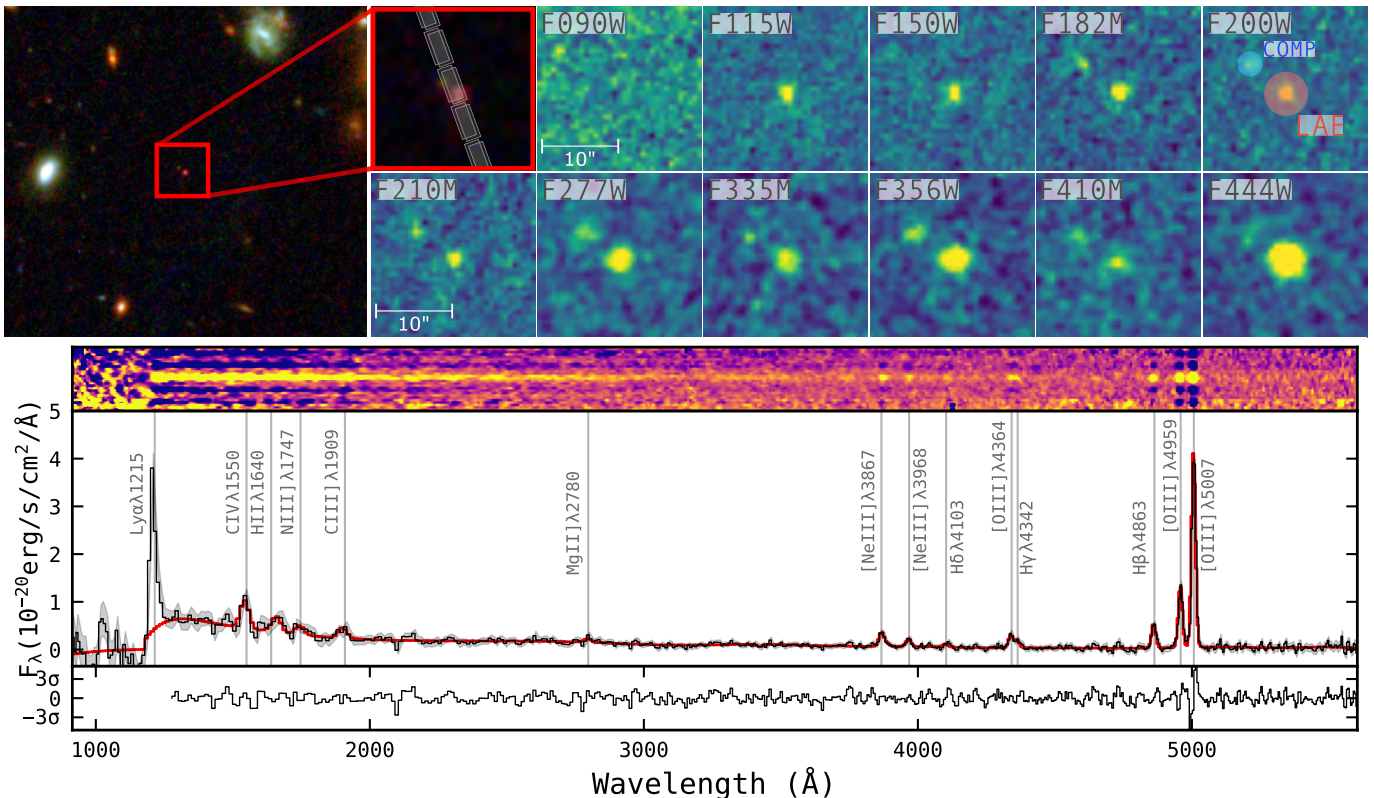


Figure 1. Top: Postage stamps centered on GN- z 8-LAE for all NIRCcam bands, together with the RGB image, and a zoom-in showing the position of the MSA shutters for prism observations. Note the presence of a close companion, marked as COMP. **Bottom:** 1D and 2D prism spectrum for GN- z 8-LAE. We show the observed spectrum as a black line and the best-fit MSAEXP model (narrow lines and continuum) in red. Vertical lines highlight the position of some bright emission lines used in this work. We do not include the Ly α fit, as we make use of an asymmetric profile as described in Sect. 3.9.

ibrated NIRSpec/MSA spectra. We complement this rich dataset with *JWST*/NIRCcam and HST imaging.

In the following sections, we will discuss in more detail the observations of GN- z 8-LAE, which is included in the JADES catalog with NIRSpec-ID 1899 and NIRCcam-ID 1010260 ($\alpha_{2000}, \delta_{2000}$: 189h11m51.86s, 62°15′25.06″).

2.1. *JWST*/NIRCcam and HST observations

We collect all *JWST* imaging from the JADES third release public *JWST*/NIRCcam data D’Eugenio et al. (2024). *HST* images for this source were retrieved from the Hubble Legacy Fields (HLF) GOODS-N public data release, as described by Whitaker et al. (2019).

We choose to extract forced photometry using Photutils (Bradley et al. 2022), using apertures of 0.″15 radius to minimize possible contamination between GN- z 8-LAE and a nearby faint, high- z source. After confirming that the position of GN- z 8-LAE is accurate in the JADES catalog, we use the centroids to perform forced photometry. We applied the aperture corrections derived by the JADES team for matching filters and aperture size, and corrected for galactic extinction as described in Navarro-Carrera et al. (2023).

We estimated the errors by placing a series of 0.″15 radius apertures around each source in blank parts of the sky. We then measured the standard deviation between the recovered fluxes, which is the 1σ uncertainty for our flux measurements. We use 3σ uncertainties as upper limits and set the flux to zero in the case of non-detection.

As a sanity check, we compared our photometry against the one in the JADES catalog (D’Eugenio et al. 2024). All our flux measurements are in agreement with the ones reported by JADES, within their respective uncertainties.

We explore the morphology of GN- z 8-LAE by modeling it for several NIRCcam bands, covering the rest-frame UV and optical. We used both Sérsic (Sérsic 1963), Gaussian, and point-like PSF-convolved models, and fitted them to the NIRCcam observations using PetroFit (Geda et al. 2022) with PSFs generated using WebbPSF (Perrin et al. 2014) in a 3x3″ background subtracted cutout centered around GN- z 8-LAE.

Our findings suggest that GN- z 8-LAE is only resolved in the short wavelength (SW) bands, with an effective radius of 143 ± 15 pc (measured in F150W, correspond-

ing to the rest-frame UV of GN-*z*8-LAE). The fit residuals for the long wavelength (LW) bands show a good fit and do not show significant differences when using Sérsic, Gaussian, or point-like profiles (suggesting an effective radius < 190 pc).

A visual inspection of GN-*z*8-LAE highlights the presence of a faint source very close in projection to GN-*z*8-LAE, $3.''5$ in the detector plane. This galaxy is part of the JADES photometric catalog but does not have any spectroscopic observations associated with it, and could be a fainter high-*z* candidate. Fig. 1 shows the orientation of the shutters relative to GN-*z*8-LAE, together with $22''$ cutouts for all NIRC*am* bands centered in GN-*z*8-LAE (labeled as LAE). We also highlight the companion located north-west of GN-*z*8-LAE (labeled as COMP).

2.2. NIRSpec/MSA observations

We use NIRSpec/MSA spectroscopic observations from the JADES NIRC*am*+NIRSpec program in the GOODS-N (PID: 1181, PI: Eisenstein). The data are publicly available in the MAST (DOI: [10.17909/8tdj-8n28](https://doi.org/10.17909/8tdj-8n28)).

The observations of our target were taken in two different configurations: low-resolution ($R \sim 100$) using prism and covering the spectral range $0.6\text{--}5.3 \mu\text{m}$, and medium-resolution ($R \sim 1000$) using the G140M, G235M, and G395M gratings. We refer the reader to D'Eugenio et al. (2024) for a more detailed description of the observation strategy and reduction of the spectroscopic data used in this paper.

The NIRSpec observations are comprised of a total of two dithers with the 3-point nodding pattern. This translates into 12 integrations and a total of 12ks for the prism observations, and 6 integrations and a total of 6ks for each grating. This allows us to detect both strong (and faint) emission lines and continuum in the case of prism observations.

This source was not affected by any of the technical issues described in D'Eugenio et al. (2024), and the extracted spectrum has a good S/N, so no re-extraction was performed with a smaller number of pixels (e.g., 3 central pixels in Bunker et al. 2023; Witstok et al. 2024a).

We use a modified version of MSAEXP (Brammer 2023) line fitting algorithm to measure the line fluxes, their respective uncertainties, and observed equivalent widths for both prism and gratings. Among the additional features, our modified version of MSAEXP allows for broad emission line templates, and an enriched list of emission lines (Kokorev et al. 2024b in prep). MSAEXP provides a fit for all emission lines and continuum simultaneously.

It makes use of single narrow and/or broad templates for emission lines and splines for the continuum. The template matrix is fitted using least squares. We determine the upper limits using the MSAEXP best-fit continuum and the observed flux and errors, assuming the typical line width for the rest of lines in each spectrum.

We have compared our extracted line fluxes with the ones quoted in the JADES catalog. The line fluxes are in excellent agreement for all measurements in common, well within the estimated uncertainties. These values are provided in Table 1. A detailed analysis of the Ly α emission line is presented in Sect. 3.9.

3. PHYSICAL PROPERTIES OF GN-*z*8-LAE

In the following sections, we will characterize the emission lines detected for GN-*z*8-LAE, its spectroscopic redshift and UV properties, metallicity, elemental abundances and several other parameters.

We report a summary of all physical properties derived for GN-*z*8-LAE in Table 3.

3.1. Emission lines and spectroscopic redshift

The combination of broad spectral coverage and high signal-to-noise from the prism spectrum allows us to detect a wealth of rest-frame optical and UV emission lines (see Table 1). The continuum is also well-detected at all wavelengths. Fig. 1 shows both 2D and 1D spectra, the aspect of GN-*z*8-LAE in JWST/NIRC*am* images, and the positioning of the NIRSpec/MSA shutters.

We report line flux measurements and rest-frame equivalent widths (henceforth abbreviated EW_0) in Table 1. When available, we report the measured fluxes from both prism and gratings. Notably, EW_0 s are always measured using the PRISM spectrum, as the continuum is not present in gratings.

Interestingly, blue-wards of Ly α we tentatively detect an emission feature that falls at the expected wavelength of the line complex O VI $\lambda\lambda$ 1032, 1038 + Ly β + C II $\lambda\lambda$ 1036, 1037. However, a careful analysis of the spectral data reduction and extraction should be performed to confirm the presence of these lines more robustly.

The low spectral resolution of the prism observations ($R \sim 100$) makes several lines appear partially or completely blended. This is shown in Table 1. Crucially, the blending between H γ and [O III] λ 4363 is only partial, and the respective line fluxes were recovered by a careful fit in which the line central wavelengths were fixed. As a sanity check, the comparison between the deblended H γ flux, and the one from the grating spectrum shows an excellent agreement.

Table 1. Line fluxes for GN-*z*8-LAE, expressed in units of 10^{-20} erg s $^{-1}$ cm $^{-2}$

Line	FLUXPRISM	ERRORPRISM	FLUXGRATING	ERRORGRATING	EW ₀
C IV] λ 1548,1550	228	36	-	-	52.1 ± 9.3
O III] λ 1660,1666 + He II λ 1640 ^a	131	43	-	-	37 ± 13
(He II λ 1640) ^a	<35	-	-	-	-
N III] λ 1749-1753	69	30	-	-	25 ± 11
C III] λ 1907,1909	69	28	-	-	36 ± 13
Mg II λ 2795,2802	25	13	-	-	16.3 ± 9.1
[O II] λ 3726,3729 ^b	< 25	-	21	12	-
[Ne III] λ 3869 ^c	-	-	59.8	9.7	-
[Ne III] λ 3967 + H ϵ	35.0	7.0	-	-	55 ± 12
H δ	15.4	7.0	19.8	7.6	28 ± 14
H γ ^d	45	10	44	12	161 ± 27
[O III] λ 4363 ^d	28.6	9.5	-	-	97 ± 21
H β	93.1	8.0	76	12	256 ± 23
[O III] λ 4959	230	10	232	17	472 ± 21
[O III] λ 5007	715	14	749	23	1357 ± 26

^aHe II λ 1640 and O III] λ 1660,1666 are partially blended in the prism spectrum. We attempted to deblend the three line fluxes by fixing the line centers according to the spectroscopic redshift, the widths to the average one for all other (narrow) lines. However, we could only robustly set a (3σ) upper limit on the He II λ 1640, as this line is marginally separated from the O III] λ 1660,1666 doublet. None of the lines have coverage from any of the gratings. When using the O III] λ 1660,1666 flux for further calculations we consider the total He II λ 1640 + O III] λ 1660,1666 and the upper limit on the He II λ 1640 to derive a reasonable interval, including it as part of the error for all quantities.

^bNot detected in the prism spectrum, we quote the 3σ upper limit. A hint of detection is present in the grating but with low signal-to-noise.

^c[Ne III] λ 3869 is fully blended with H8 and He I λ 3889 in the prism spectrum. Only [Ne III] λ 3869 is detected in the grating.

^dH γ and [O III] λ 4363 are partially blended in the prism spectrum. However, both lines can be deblended by a careful line fit fixing the center of the lines. This is important for [O III] λ 4363, as it is not detected in the grating spectrum. Notably, the deblended and grating H γ line fluxes are in good agreement.

The spectroscopic redshift of GN-*z*8-LAE was derived by averaging the positions of all emission lines detected in the prism spectrum (excluding blended lines and the Ly α line). We report a redshift $z_{spec} = 8.2790 \pm 0.0005$. This spectroscopic redshift solution derived using NIR-Spec/MSA is in good agreement with the one obtained by the FRESCO team using only the [O III] λ 5007,4959 lines ($z_{spec} = 8.28$ Oesch et al. 2023)) and with the one reported by Witstok et al. (2024a).

Wavelength calibration offsets between prism and grating spectra were reported by D'Eugenio et al. (2024), thus we double-checked the spectroscopic redshift obtained from grating G395M, with the most detected emission lines. We retrieved a $z_{spec} = 8.279 \pm 0.002$, compatible with the PRISM solution. The peak of the [O III] λ 5007 from the G395M is in excellent agreement with the redshift determined from the prism spectrum (see Fig. 6). Accordingly, no systematic effect on

wavelength calibration was found between gratings and prism for GN-*z*8-LAE.

3.2. Spectro-photometric SED fitting

To fully explore the high-quality photometric and spectroscopic data available for GN-*z*8-LAE, we use BAGPIPES (Carnall et al. 2019a) for performing a joint spectro-photometric SED fitting. Table 2 lists the configuration parameters employed for the run. Briefly, BAGPIPES uses stellar emission from Bruzual & Charlot (2003) with an Kroupa (2001) initial mass function (IMF) with a cut-off mass of $120 M_{\odot}$, and nebular emission from CLOUDY (Ferland et al. 2013). We used broad and flat (uninformative) priors for all parameters, as the combination of spectrum and photometry has enough constraints without any additional information. All runs were performed by fixing the redshift to the spectro-

Table 2. Quantities derived using the spectro-photometric BAGPIPES SED fit, and their respective priors.

Parameter	Reference/Prior	Best-fit Value
Templates	BC03 ^a	
SFH	delayed exponential	
e -folding time (τ , Gyr)	0.0001–15	0.06 ± 0.06
Mass ($\log_{10} \mathcal{M}/\mathcal{M}_{\odot}$)	1 – 13	7.66 ± 0.02
Metallicity (Z/Z_{\odot})	0.001 – 1	0.2 ± 0.01
Age (Gyr)	0.0001 – 15	0.001 ± 0.001
$\log U$	–4 – –0.5	-1.0 ± 0.12
Extinction law	SMC ^c	
A_v	0.0 - 7.0	0.03 ± 0.02
β -slope	-	-2.5 ± 0.1
IMF	Kroupa (2001)	

^a2016 version of Bruzual & Charlot (2003)

^cGordon et al. (2003)

scopic value retrieved as described in the previous sections.

We use the techniques described by Carnall et al. (2019b) to take full advantage of the combination of spectroscopic and photometric datasets. In particular, we allow for a $< 2\sigma$ perturbation to the spectrum in the form of a second-order Chebyshev polynomial, which can correct for systematic issues in the flux calibration, although we found the applied correction to be small in the case of GN- z 8-LAE. We also allow for a multiplicative factor on the spectroscopic errors to correct for underestimated uncertainties. These new parameters are fitted simultaneously to the rest of the physical parameters.

The best-fit results are shown in Table 2, assuming a delayed exponential star formation history (see Schaerer et al. 2024). They indicate that GN- z 8-LAE has a low stellar mass ($\mathcal{M} \sim 10^{7.66}$), is extremely young (best-fit age of ~ 10 Myr), and has low dust extinction ($E(B - V) \sim 0.02$). The metallicity we retrieve is approximately 1/5th solar ($12 + \log(O/H) \sim 8$). Finally, the ionization parameter is elevated, with $\log U \sim -1$.

These parameters appear to be in broad agreement with the ones derived from direct spectroscopic measurements for GN- z 8-LAE (Table 3) and other high- z LAEs (Table 5) and low- z LAEs (Ouchi et al. 2020).

3.3. UV magnitude and slope from the NIRSpect spectrum

We measure an UV-magnitude of $M_{UV} = -19.55 \pm 0.22$ at 1500 \AA and UV β -slope $\beta = -2.48 \pm 0.23$ (us-

ing the best-fit continuum and the definition by Calzetti et al. 1994). This places GN- z 8-LAE close to the typical M_{UV}^* at $z \sim 8$ (e.g., Bouwens et al. 2021; Donnan et al. 2023), making GN- z 8-LAE relatively bright compared to similar LAEs (e.g., Saxena et al. 2023). Additionally, we retrieve the values for M_{UV} and UV β slope from NIRCcam+*HST* photometry. We recover $M_{UV} = -19.59 \pm 0.15$ and $\beta = -2.73 \pm 0.35$. The agreement in M_{UV} ensures that there is no significant systematic offset between photometry and spectrum (e.g., due to uncertainties in path-loss corrections Kokorev et al. 2023). The departure in the β values can be explained by the photometry being affected by strong UV emission lines.

When comparing to the median value of high- z LAEs and SFGs samples studied using *JWST* (Table 5, Kumari et al. 2024; Morishita et al. 2024; Iani et al. 2024b) or the general population of $z > 6$ galaxies (Bouwens et al. 2009), GN- z 8-LAE shows a bluer UV β -slope. Several studies link blue β slopes (and absence of dust) to an enhanced f_{esc}^{LyC} (e.g., Chisholm et al. 2022).

As a sanity check, the values for spectroscopic redshift, M_{UV} and β slope derived in our analysis are in good agreement with the ones reported by (Witstok et al. 2024a). Our β slope is slightly bluer but in agreement within the errors (this discrepancy could be rooted in the different techniques we used to fit the FUV continuum). Our values for emission line fluxes are in good agreement with the ones reported in the JADES catalog (D’Eugenio et al. 2024). The measurements reported by Witstok et al. (2024a) for GN- z 8-LAE are systematically smaller when compared to the ones from JADES and our study. This difference could be explained by the different extraction procedures used by Witstok et al. (2024a).

3.4. Basic physical properties from the NIRSpect spectrum

We estimate the color excess $E(B - V)$ by inspecting the Balmer decrement between $H\gamma$ and $H\beta$ (using theoretical values from Storey & Hummer 1995). We use an SMC (Gordon et al. 2003) extinction law for all our $E(B - V)$ measurements. Accordingly, we recover a color excess of $E(B - V) = 0.02 \pm 0.38$. Together with the insights from the β slope (Meurer et al. 1999) and BAGPIPES, all three estimators converge towards the low dust content of GN- z 8-LAE. This is in line with the results for strong $Ly\alpha$ emitters in the literature (e.g., Rosani et al. 2020; Saxena et al. 2023). For all the reasons above, we do not apply any dust correction to line ratios, fluxes, or derived quantities in this paper.

Table 3. Summary of the physical properties of GN-z8-LAE

Quantity	Value	Section
z	8.2790 ± 0.0007	§3.1
M_{UV} (mag)	-19.6 ± 0.3	§3.3
β	-2.48 ± 0.23	"
$E(B - V)$ (mag)	0.02 ± 0.38	§3.4
$\log_{10}(M^*/M_{\odot})^{\dagger}$	7.66 ± 0.02	§3.2
R_{eff}^{UV} (pc)	143 ± 15	§2
$\text{SFR}_{H\alpha}$ (M_{\odot})	11.3 ± 7.8	§3.4
SFR_{UV} (M_{\odot})	3.0 ± 2.1	"
age (Myr)	2 – 6	"
Σ_{M^*} (M_{\odot}/pc^2) [†]	355 ± 75	§3.8
$\Sigma_{\text{SFR}(H\beta)}$ ($M_{\odot}/\text{yr}/\text{kpc}^2$)	88 ± 32	§3.8
T_e (K)	$(1.73 \pm 0.24) \times 10^4$	§3.5
$12 + \log(\text{O}/\text{H})_{\text{mean}}^{\ddagger}$	7.85 ± 0.17	"
$\log(\text{C}/\text{O})$	-0.69 ± 0.21	§3.7
$\log(\text{N}/\text{O})$	-0.44 ± 0.36	§3.8
$F_{Ly\alpha}$ ($10^{-20} \text{ erg s}^{-1} \text{ cm}^{-2}$) [*]	753 ± 56	§3.9
$\text{EW}_0^{Ly\alpha}$ (\AA) ^{**}	235 ± 10	"
$\Delta v_{Ly\alpha}$ (km/s)	132 ± 72	"
$f_{\text{esc}}^{Ly\alpha}$	0.25 – 0.40	"
$f_{\text{esc}}^{LyC^{***}}$	$\sim 60\%(14\%)$	§4.2
$\log \xi_{\text{ion}}^0$	25.78 ± 0.31	§4.3

[†]Stellar mass derived using spectro-photometric BAGPIPES SED fit, see Tab. 2.

[‡]Average value between direct (T_e based method) and optical metallicity calibrations, see Tab. 4.

^{*}From the best-fit asymmetric model (Shibuya et al. 2014) flux for the G140M spectrum.

^{**}Derived using the prism spectrum, see 3.9.

^{***}Average value for all estimators used in Sect. 4.2, in brackets the smallest value.

Under the assumption that all emission lines originate from the reprocessing of ionizing photons from young, short-lived massive stars in the ISM of the galaxy (see Sect. 3.6), it is possible to estimate the instantaneous star formation rate (in the past 10 Myr) from the luminosity of Balmer lines (Kennicutt 1998; Rinaldi et al. 2023) after taking into account the Kroupa (2001) IMF we use in this work.

As the PRISM spectrum does not cover $H\alpha$ we derive the SFR from the $H\beta$ flux instead, by applying the relations by Storey & Hummer (1995). By doing so, we retrieve $L_{H\alpha} = (2.14 \pm 0.18) \times 10^{42}$ erg/s, which in turn corresponds to $\text{SFR}_{H\alpha} = 11.3 \pm 7.8 M_{\odot}/\text{yr}$, where

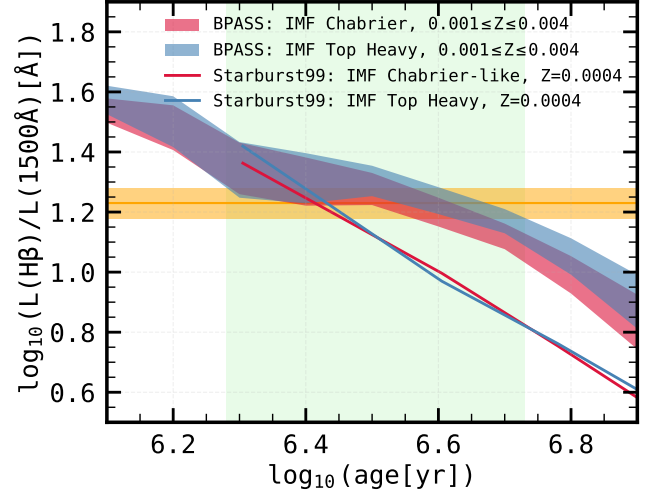


Figure 2. Constraint on the light-weighted age of our target source based on the $H\beta$ luminosity and FUV(1500 Å) luminosity density ratio. We include theoretical tracks for a single burst SFH (since the onset of star formation) for BPASS (v2.2.1 Eldridge et al. 2017, as shaded areas, between $0.001 < Z < 0.004$) and Starburst99 (Leitherer et al. 1999, as continuous lines for a fixed $Z = 0.0004$). These tracks are derived for Chabrier-like and Top-heavy IMF with a cut-off mass of $300 M_{\odot}$, color-coded in red and blue, respectively (see Sect. 3.8). The age range compatible with the line luminosity ratio measured for GN-z8-LAE (orange line) is shown as a green-shaded area.

the error incorporates in quadrature the intrinsic scatter inherent to the Kennicutt (1998) calibration.

If deriving the SFR from FUV luminosity density (Kennicutt 1998), the ratio $\text{SFR}_{H\alpha}/\text{SFR}_{UV}$ takes the value $\log_{10} \text{SFR}_{H\alpha}/\text{SFR}_{UV} = 0.57 \pm 0.42$. As discussed by Weisz et al. (2012); Faisst et al. (2019); Emami et al. (2019) and Navarro-Carrera et al. (in prep.), the ratio $\text{SFR}_{H\alpha}/\text{SFR}_{UV}$ is a tracer of recent burstiness in the star formation history. Ratios $\log_{10} \text{SFR}_{H\alpha}/\text{SFR}_{UV} \gtrsim 0.2$ indicate a very recent burst in star formation, produced not longer than 50 Myr ago.

GN-z8-LAE shows a $\text{SFR}_{H\alpha}/\text{SFR}_{UV}$ well above unity. This is in agreement with predictions from simulations (Sparre et al. 2017; Ceverino et al. 2018) and observations (Navarro-Carrera et al., in prep.), where low-mass galaxies are expected to show increasingly bursty SFHs and, thus, populate the starburst cloud (Rinaldi et al. 2024b). The expected light-weighted age for GN-z8-LAE is extremely young: ≤ 50 Myr.

The specific star formation rate (sSFR) of GN-z8-LAE is $\log_{10} \text{sSFR}_{H\alpha}/\text{yr}^{-1} = -6.55 \pm 0.30$. Following the criterion from Caputi et al. (2017, 2021), GN-z8-LAE is classified as a starburst (SB) galaxy, as $\log_{10} \text{sSFR}/\text{yr}^{-1} \gg -7.6$.

Table 4. Values of electron temperature and gas-phase metallicity from the direct method, UV, and optical calibrations.

Calibration	$12 + \log \text{O}/\text{H}$	Reference
Direct $T_e = (17 \pm 0.2) \times 10^3 \text{K}$	$(7.77 - 7.79) \pm 0.14$	I06 ^a
C3O3	$(7.12 - 7.20) \pm 0.27$	M22 ^b
EWCIII	7.20 ± 0.24	M22 ^b
R23	$(7.86 - 8.03) \pm 0.10$	S24 ^c
O3	7.92 ± 0.10	S24 ^c

^aI06, (Izotov et al. (2006)).

^bM22, (Mingozzi et al. 2022).

^cS23, (Sanders et al. 2024).

By further exploring the relation between the Balmer lines and the UV luminosity density it is possible to estimate a value for the light-weighted age, under the assumption of GN-*z*8-LAE being a star-forming galaxy. We explore the evolution of stellar tracks from **Starbust99** (Leitherer et al. 1999) and **BPASS** (v2.2.1 Eldridge et al. 2017; Stanway & Eldridge 2018) for Chabrier-like and top-heavy IMFs (the uncertainty on our measurements is much larger than the one produced by the choice of IMF). We then explore the time-evolution of the ratio between $L_{\text{H}\beta}$ and L'_{1500} . We refer the reader to Iani et al. (2022b) for an in-depth discussion of the methodology. For GN-*z*8-LAE we found a light-weighted age in the range of 2 – 6 Myr, as shown in Fig. 2.

All properties are in line with the ones obtained in the analysis by Witstok et al. (2024a). We infer lower dust content and slightly higher instantaneous SFR (both compatible within the uncertainty).

Having reviewed the basic properties of GN-*z*8-LAE, in the following sections, we will overview in more detail our derivations for gas-phase metallicity, ionization source, and C and N abundances.

3.5. Auroral line determination of electron temperature, and gas-phase metallicity

By following Proxauf et al. (2014), we constrain the $T_e(\text{OIII})$ (hereafter T_e) of the ionized gas thanks to the presence of the auroral $[\text{O III}] \lambda 4363$ line (ruled by collisional excitation). In particular, we use the ratio $([\text{O III}] \lambda 4958, 5007)/[\text{O III}] \lambda 4363$, which is monoton-

ically correlated to T_e . For GN-*z*8-LAE, we report $T_e = (1.73 \pm 0.24) \times 10^4 \text{K}$.

We use a variety of UV and optical calibrations for determining the gas-phase metallicity of GN-*z*8-LAE, together with the estimation from the direct (T_e) method (Sanders et al. 2024; Izotov et al. 2006). For the so-called direct method, we consider that $\text{O}/\text{H} = \text{O}^+/\text{H}^+ + \text{O}^{++}/\text{H}^+$ by assuming the rest of higher ionization terms to be negligible (Sanders et al. 2024). We use the calibrations from Izotov et al. (2006) to derive O^+/H^+ and O^{++}/H^+ . The term O^+/H^+ directly depends on the $[\text{O II}] \lambda \lambda 3727/\text{H}\beta$ ratio, for which we have only an upper limit. We report the derived metallicity as an interval.

All the values for metallicities are displayed in Table 4. We find an average value of $12 + \log \text{O}/\text{H} = 7.85 \pm 0.17$ or $Z = (0.14 \pm 0.05)Z_\odot$ (Asplund et al. 2021) as an average between the two optical diagnostics and the direct method. The discrepancy between optical/direct metallicities and UV metallicities could be due to the strong dependence of UV lines on the ionization of the ISM (Maiolino & Mannucci 2019).

By inspecting Table 5, GN-*z*8-LAE is slightly more metal-rich when compared to typical LAEs or N-emitters at similar redshifts (Kumari et al. 2024; Schaerer et al. 2024; Topping et al. 2024). However, we find it consistent with the SFGs population (Kumari et al. 2024) and with the expectations from the mass-metallicity relation (MZR, although slightly above the median trend reported by Curti et al. 2024).

3.6. The ionization source

The presence of UV emission lines is usually associated with hard ionization fields and ionization parameters in the range $\log U \geq -2.5$ ¹, coupled with relatively low gas-phase metallicity ($12 + \log(\text{O}/\text{H}) \leq 8.3$) (Jaskot & Ravindranath 2016; Mingozzi et al. 2024). The presence of strong high-ionization lines such as $\text{C IV}] \lambda 1548, 1550$ in the spectrum of GN-*z*8-LAE (highly likely from nebular origin) strengthens this idea.

The $[\text{O III}] \lambda 5007/[\text{O II}] \lambda \lambda 3727$ ratios probe intermediate-ionization regions. By using UV diagnostics calibrated for these regions (Mingozzi et al. 2022), we get $\log U = -1.36 \pm 0.5$ from $\text{EW}_0(\text{C IV}] \lambda 1549)$, and $\log U = -1.35 \pm 0.32$ from $\text{C IV}] \lambda 1548/\text{C III}] \lambda 1907$. These values are compatible with the one derived in

¹ $\log U$ is defined as the ratio between the number density of ionizing photons and the number density of hydrogen atoms (e.g., Osterbrock & Ferland 2006)

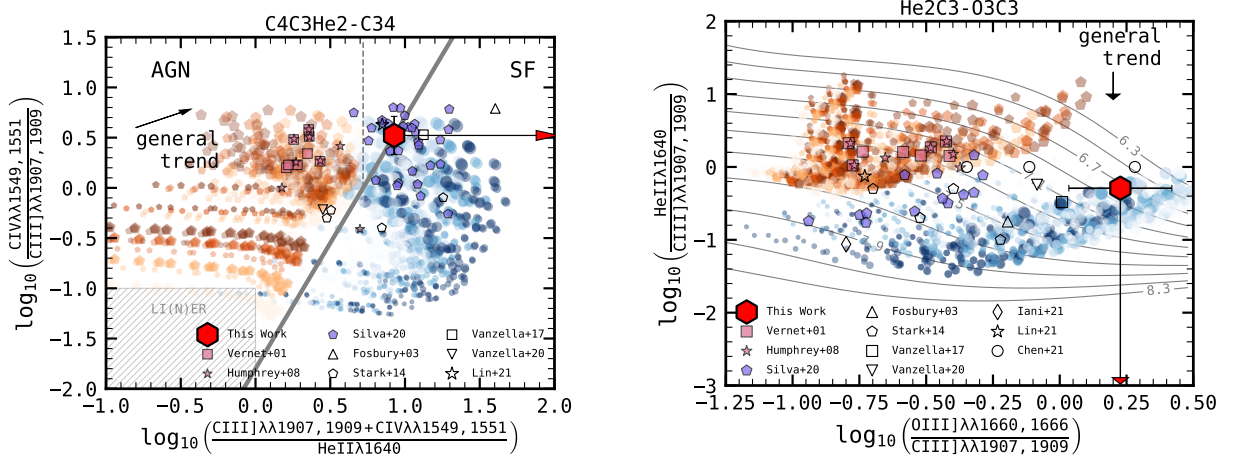


Figure 3. Left/Right: The C4C3He2-C34/He2C3-O3C3 line diagnostics (Nakajima et al. 2018) that discriminate between AGN and SF-dominated ionized regions. The values for GN-z8-LAE are shown as a red hexagon (with the upper limit on the He II). Together with this, we include the AGN and SFG by Feltre et al. (2016) (F16) and Gutkin et al. (2016) (G16) as red and blue markers, respectively. We show bigger markers for higher values of $\log U$, within the range $\log U - 4 \sim -0.75$. We refer the reader to Iani et al. (2022b) for a description of the literature in the figures. $\log(\text{C}/\text{O})$ abundance or UV spectral slope (α , $f_\nu \propto \nu^\alpha$) are related to the opacity of the markers, higher opacity was assigned to bigger values in both cases. We do not apply additional cuts to the F16 models shown in this work (either in their gas density or dust-to-metal mass ratios)

Table 5. Properties of some of the high- z galaxies studied with NIRSPEC, including SFGs, LAEs, and N-emitter galaxies. Indirect (e.g., best-fit derived quantities) or photometric measurements are shown between brackets.

Galaxy	z	M_{UV} (mag)	$\log M^*$ (M_\odot)	SFR (M_\odot/yr)	β	$\text{EW}_{\text{Ly}\alpha}^0$ (\AA)	$12 + \log(\text{O}/\text{H})$	R_{eff} (pc)	type	reference
GN-z8-LAE	8.279	-19.6	7.66	11.3	-2.73	203	7.85	140	LAE & N-em	This Work
GN-z11	10.6	-21.5	8.73	24	-2.4	18	7.66	64	LAE & N-em	Bunker et al. (2023)
JADES-GS-z7-LA	7.28	-17.0	6.9	0.3-0.6	-2.0	388	(8.16)	-	LAE	Saxena et al. (2023)
COLA1	6.59	-21.35	9.93	10.1	(-3.2)	-	7.88	< 260	LAE	Torralba-Torregrosa et al. (2024)
JADES LAEs	> 6.3	-19.00	-	-	-2.34	-	7.50	-	LAEs	Kumari et al. (2024)
JADES SFGs	> 6.3	-19.08	-	-	-2.26	-	7.73	-	SFGs	Kumari et al. (2024)
NIRSPEC SFGs	> 5	-19.25	8.48	3.86	-2.23	-	-	309	SFGs	Morishita et al. (2024)
GS-z14-0	14.3	-20.81	8.7	22	-2.20	-	(7.11)	260	SFG	Carniani et al. (2024)
GS-z14-1	13.9	-19.00	8.0	2	-2.71	-	(7.69)	< 160	SFG	Carniani et al. (2024)
GHz2	13.9	-20.53	9.05	5.2	-2.46	-	7.26	105	SFG	Castellano et al. (2024)
GN-z9p4	9.4	-21.00	8.7	64	-	-	7.37	118	N-em	Schaerer et al. (2024)
RXCJ2248	8.05	-20	8.05	63	-2.72	-	7.43	< 22	N-em	Topping et al. (2024)

the spectro-photometric SED fit (Sect. 3.2). When compared to the median values of $\log U$ of high- z SFGs ($z \sim 1.5 - 6$ Reddy et al. 2023a,b), GN-z8-LAE shows an enhanced $\log U$, more in line with the results of Williams et al. (2023) for an ultra-compact, magnified galaxy at $z = 9.51$.

We discard the presence of a Type I Active Galactic Nucleus (AGN) (McCarthy 1993; Ramos Almeida et al. 2011), as no evidence of broadening or wings has been found for GN-z8-LAE. This is true for both the prism

and grating spectra, with essentially all lines being unresolved ($\Delta V \leq 200$ km/s). The average measured line width for the G395M/F290LP spectrum (the one with more detected lines) is $\sim 210 \pm 175$ km/s. Moreover, no X-ray detection in the vicinity of GN-z8-LAE is reported within the 2 Ms Chandra Deep Field-North Survey catalog (Xue et al. 2016). However, we discuss the possibility of a Type II AGN in the following paragraphs.

Several UV diagnostics have been proposed to discriminate between SF or AGN-dominated galaxies. In

Fig. 3 we show two diagnostics adapted from Iani et al. (2022a)—namely C4C3-C34 and C3He2-O3C3 (e.g. Nakajima et al. 2018; Hirschmann et al. 2019; Byler et al. 2020). We overlay photoionization models for nebular emission in SFGs (as blue hexagons, Gutkin et al. 2016, G16) and AGN (red pentagons, Feltre et al. 2016, F16). We limit the models to subsolar metallicities ($Z = 0.0005 - 0.006 = (0.025 - 0.3) Z_{\odot}$).

GN-z8-LAE falls in the SF region for C4C3He2-C34 and He2C3-O3C3 (see Fig. 3), in particular, the one with the highest ionization parameter. However, it does it only marginally in the case of C4C3He2-C4C3 and also when putting it in the context of the mass-excitation diagram (MEX, Juneau et al. 2014). We also find GN-z8-LAE to be compatible with SF galaxies with the highest $\log U$ by using the O3H γ /O33 diagnostic (Mazzolari et al. 2024).

In light of these results, the ionizing radiation in GN-z8-LAE probably originated from a population of young, massive stars, rather than AGN. However, a contribution of AGN, shocks, and SF (so-called composite Hirschmann et al. 2019) can not be completely ruled out.

3.7. C/O abundance

Following Pérez-Montero & Amorín (2017), we estimate the C/O abundance from the ratio between (C III] $\lambda\lambda$ 1907,1909 + C IV] λ 1548) and O III] $\lambda\lambda$ 1660,1666) (see also Berg et al. 2016). We estimate a $\log(C/O) = -0.69 \pm 0.21$, i.e. almost half of the solar value ($[C/O]_{\odot} = 0.44$, Gutkin et al. 2016).

The value we retrieved is in agreement with those of local, metal-poor dwarf galaxies (Berg et al. 2019) and with young low-mass and low-luminosity galaxies at intermediate redshift ($z = 1.5 - 5.0$) (e.g., Erb et al. 2010; Stark et al. 2014). Our target metallicity estimate ($12 + \log_{10}(O/H) \sim 7.85$) is in agreement with the (C/O) - metallicity trend reported by (Garnett et al. 1995; Nicholls et al. 2017).

The physical origin of this trend is likely associated with the metallicity dependence of winds from massive rotating stars, along with the delayed release of carbon from lower mass stars (e.g., Henry et al. 2000; Akerman et al. 2004).

3.8. The N III] λ 1749-1753 complex

Several high- z N-emitter galaxies have been found very recently using JWST/NIRSpec: GHZ2/GLASS-z12 (Castellano et al. 2024), GN-z11 (Bunker et al. 2024; Cameron et al. 2023; Senchyna et al. 2024), GN-z9p4 (Schaerer et al. 2024), GLASS-150008 (Isobe et al. 2023), CEERS-1019 (Marques-Chaves et al. 2024),

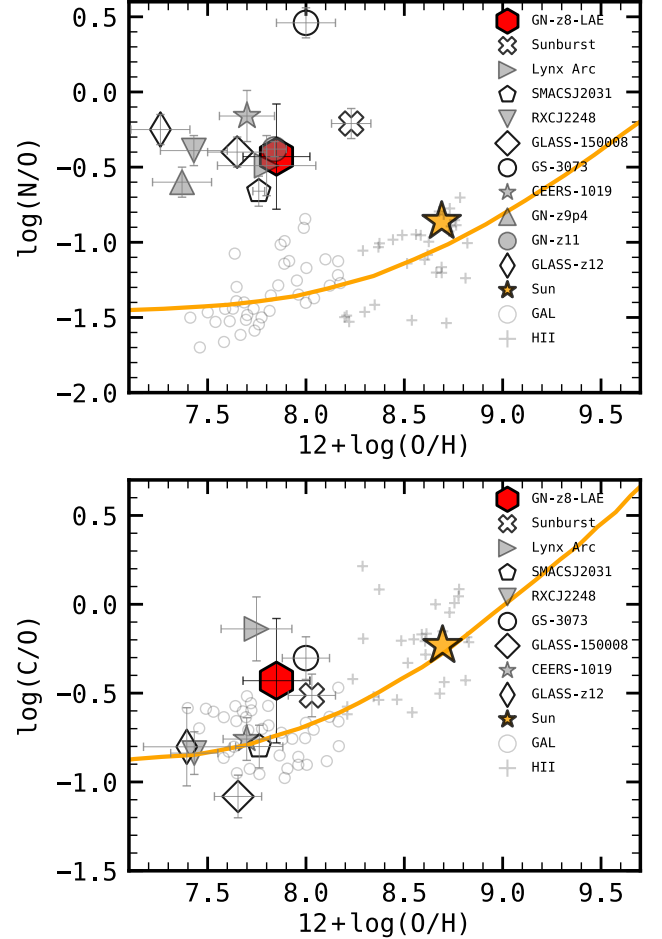


Figure 4. Top/bottom: Nitrogen/carbon over oxygen abundance as a function of metallicity, respectively. We include points for Lynx and Sunburst arc (Villar-Martín et al. 2004; Meštrić et al. 2022), all high- z N-emitters proven by NIRSpec (Marques-Chaves et al. 2024; Topping et al. 2024; Ji et al. 2024; Isobe et al. 2023; Castellano et al. 2024), and set of low-redshift HII regions and galaxies from Izotov et al. (2022). The expected trend from local studies (Vila-Costas & Edmunds 1993; Dopita et al. 2006) is shown as an orange line, and the solar values (Asplund et al. 2021) are included as an orange star.

RXCJ2248-4431 (Topping et al. 2024) and GS-3073 (Ji et al. 2024).

As reported in Table 1, we find a N III] λ 1749-1753 (blended complex of emission lines) 2.3σ detection in the PRISM spectrum of GN-z8-LAE. This would position GN-z8-LAE amongst the highest redshift N-emitter galaxies, and the only one with strong Ly α emission. When inspecting the PRISM spectrum of GN-z8-LAE we found a weak feature resembling an emission line in the expected position of N IV] λ 1486, however, it is not possible to constrain it further due to its low signal-to-noise.

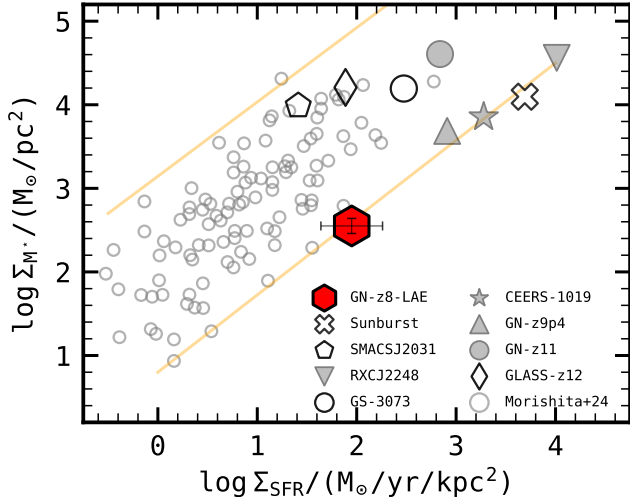


Figure 5. Stellar mass surface density as a function of star formation rate surface density. Here, GN-z8-LAE is shown as a red hexagon. We include the Sunburst arc (Meštrić et al. 2022) and all high- z N-emitters proven by NIRSspec (Marques-Chaves et al. 2024; Topping et al. 2024; Ji et al. 2024; Isobe et al. 2023; Castellano et al. 2024). The orange lines mark the sSFR envelope for SFGs and N-emitters, and portrays GN-z8-LAE with the maximum sSFR together with some of the N-emitters, that have higher stellar mass.

By using the relations from (Villar-Martín et al. 2004; Aller 1984), we derived $\log(N^{2+}/H^+) = -4.6 \pm 0.3$ directly from our measurement of N III] $\lambda 1749-1753/H\beta$. As we do not have any detection of higher ionization N lines (N IV] $\lambda 1486$), we use the relations by Hamann et al. (2002) for the metallicity of GN-z8-LAE to predict the N IV] $\lambda 1486$ flux from our C IV] $\lambda 1548, 1550$ measurement. This allows us to determine $\log(N^{3+}/H^+) = -6.4 \pm 0.4$. The total Nitrogen abundance is dominated by the contribution of the direct measurement of N^{2+}/H^+ , so the assumptions behind the determination of N^{3+}/H^+ could only further increase the Nitrogen abundance.

All in all, we derive an elevated, super-solar Nitrogen abundance of $\log(N/H) = -4.58 \pm 0.36$ and, in turn, $\log(N/O) = -0.44 \pm 0.36$ for GN-z8-LAE. In particular, this ratio translates to approximately 2.8 times the solar ratio (Asplund et al. 2021). This is in line with other high- z N-emitters compact SFGs, characterized by an N-enriched (with supersolar N abundances) and metal-poor (low-metallicity, O/H) ISM (Marques-Chaves et al. 2024).

As of today, no unique scenario exists to interpret the presence of N lines and reconcile the super-solar nitrogen abundance in metal-poor galaxies. Wolf-Rayet stars, very massive and supermassive stars ($M^* > 100 M_\odot$), a top-heavy IMF, and tidal disruption events have been

suggested as mechanisms that could enhance the nitrogen abundance (see Schaerer et al. 2024, and references therein).

In the case of GN-z8-LAE, the strong high-ionization lines, Ly α and N III] $\lambda 1749-1753$, seem to favor the scenario of a short burst of intense star formation in the present or past few million years (Topping et al. 2024). This is in agreement with our findings in Sec. 3.2 and 3.

Taking advantage of the morphological properties we derived in 2, we can study the position of GN-z8-LAE in the stellar mass surface density (Σ_M^*) - star formation surface density (Σ_{SFR}) plane, shown in Fig. 5. We report these results in Table 3, following Reddy et al. (2023a) and using the SFR derived from the Balmer lines and the stellar mass from the spectro-photometric fit reported in Table 2.

In Fig. 5 we include the compilation of spectroscopically confirmed SFGs at $z > 5$ by (Morishita et al. 2024), and all the known Nitrogen emitters discovered with NIRSspec (see Sect. 3.8). From the position in this plane, GN-z8-LAE shows a smaller stellar mass surface density compared to the rest of N-emitters, and is located in the extreme sSFR envelope of the SFG distribution (again, as several other N-emitters).

3.9. The Ly α emission of JADES-GN-z8-LA

GN-z8-LAE was selected as a strong Ly α emitter, as can be seen in Fig. 1. We detect Ly α in both prism and the G140M grating spectra with a signal-to-noise of approximately 12 in both cases.

We model the Ly α line using an asymmetric profile as proposed by Shibuya et al. (2014). We report a flux of $F_{Ly\alpha} = (753 \pm 56) \times 10^{-20}$ erg/s/cm 2 for the G140M grating. We also report a $EW_0 = 235 \pm 10$ Å. Note that this value was derived using the prism spectrum, where the spectral continuum is detected.

From the best-fit Ly α model, we report a velocity offset of $\Delta v_{Ly\alpha} = 133 \pm 72$ km/s with respect to the systemic velocity of the system. This value is small, within the line spread function of NIRSspec around $1 \mu\text{m}$ (Saxena et al. 2023), but similar to the one reported by Saxena et al. (2024) for several LAEs and also compatible with values from the compilation of $z > 5.8$ LAEs by Witstok et al. (2024b). The presence of Ly α emission close (or at) the systemic velocity could indicate a low neutral hydrogen column density over the line-of-sight (LOS Kerutt et al. 2024).

The Ly α line is not resolved in the prism spectrum, and we find a similar situation for the G140M grating (Fig. 6). We recover a best-fit line width comparable to the spread function (LSF), of ~ 200 km/s.

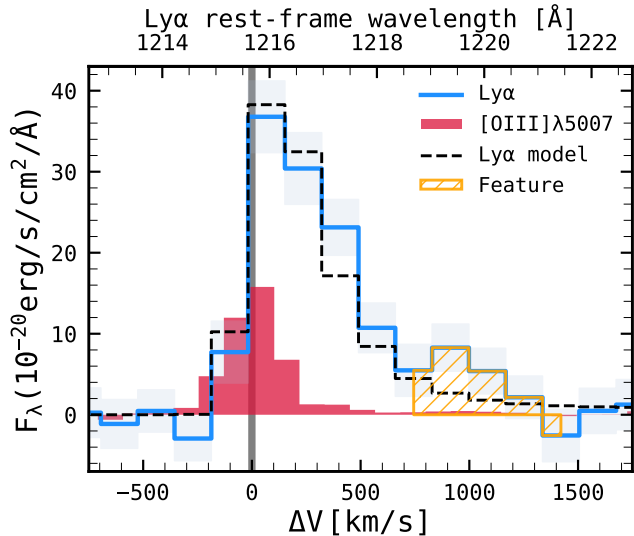


Figure 6. The Ly α line from the grating (G140M) spectrum in velocity space (blue line). The asymmetric model from Shibuya et al. (2014) is shown as a dashed black line. Relative to it, the O III] $\lambda\lambda 5007$ line profile from the G395M grating observations is shown as a red area. The orange hatched area highlights the emission feature investigated in Sect. 3.9.

The flux recovered from the prism spectrum is $F_{\text{Ly}\alpha} = (871 \pm 82) \times 10^{-20} \text{ erg/s/cm}^2$. This value is enhanced with respect to the model flux from the G140M grating. We explain this by the presence of a feature red-wise of the Ly α line. This feature is blended with Ly α for the prism observations, but can be resolved using the G140M grating, as shown in Fig. 6 (orange hatched area). We found several possible explanations for this feature assuming it is not a random fluctuation: 1. A broad red wing associated with the Ly α line (Yang et al. 2014). 2. An effect of the O V]1218 emission line (Humphrey 2019; Iani et al. 2022a). 3. An effect of Ly α scattering.

Several arguments disfavor the possibility of the feature being O V]1218 emission. First of all, we find no evidence of the presence of the remaining component of the doublet O V] $\lambda\lambda 1214, 1218$. O V]1214 is expected to be brighter than O V]1218 from models (Humphrey 2019) and it is far enough from Ly α to be resolved in the G140M spectrum. Perhaps more importantly, we found the line center associated with O V]1218 not to be in agreement with the systemic redshift of GN-*z*8-LAE.

The specific shape of the Ly α profile is expected to depend on the conditions of both intergalactic medium (IGM) and ISM (Blaizot et al. 2023; Witten et al. 2023, 2024). However, a detailed modeling of the Ly α profile falls out of the scope of our analysis.

By comparing the ratio between the observed Ly α flux, and Balmer lines to theoretical predictions, we can estimate the Ly α escape fraction (although with caveats, see Choustikov et al. 2024b). We assume a Case B recombination and an electron density between 100 cm^{-3} and 1000 cm^{-3} and use the electron temperature derived in Sect. 3.5. Using PyNeb (Luridiana et al. 2015), we derive $F_{\text{Ly}\alpha}/F_{\text{H}\beta} = 25.68 - 31.80$, for 100 cm^{-3} and 1000 cm^{-3} , respectively. By comparing this ratio with the one observed in GN-*z*8-LAE we retrieve a $f_{\text{Ly}\alpha}^{\text{esc}} = 0.25 - 0.40$. Any dust correction would shift $f_{\text{Ly}\alpha}^{\text{esc}}$ towards higher values.

Our derived $f_{\text{Ly}\alpha}^{\text{esc}}$ is in agreement with the one found by using indirect tracers (e.g., $\text{EW}_0^{\text{Ly}\alpha}$, β and ξ_{ion} Sobral & Matthee 2019). In particular, we employ the relation corrected for the ionizing photon production efficiency (see Sect. 4.3) and dust extinction from Sobral & Matthee (2019, Eq. 6) to retrieve $f_{\text{Ly}\alpha}^{\text{esc}} = 0.63 \pm 0.31$. This value is compatible with the direct method estimations within the error bars.

Our retrieved value for the Ly α escape fraction is reasonable when comparing it to a sample of LAEs at $5.8 < z < 7.98$ selected from JADES NIRSPec observations (Witstok et al. 2024b). In particular, an enhanced $f_{\text{Ly}\alpha}^{\text{esc}}$ could also be linked to an enhanced $f_{\text{LyC}}^{\text{esc}}$ (Chisholm et al. 2018; Naidu et al. 2022).

4. GN-*z*8-LAE AS A LyC LEAKER

Young and star-forming galaxies such as GN-*z*8-LAE are expected to produce a high number of ionizing photons, but only the ones that escape the galaxy (i.e., are not absorbed in ISM) effectively contribute towards the reionization of the universe (Chisholm et al. 2020). In particular, LyC leakers are defined by having a non-negligible escape of LyC photons.

Two scenarios for the escape of LyC photons have been proposed, even though low-mass/faint and star-forming galaxies are rich in neutral hydrogen, which is opaque to LyC radiation (e.g., Watts et al. 2021). The density-bounded medium scenario involves the presence of a low-column-density neutral hydrogen medium surrounding the sources of ionizing radiation. Some authors have suggested that it fails to reproduce spectral properties of LyC leakers (Ramambason et al. 2020).

The second scenario consists of the presence of an optically thick but porous medium, that does not completely cover all the sources of ionizing radiation (Zackrisson et al. 2013). Following Rivera-Thorsen et al. (2017), we divide this second scenario into two cases: one where the medium is clumpy and provides a multitude of clear LOS (picket fence model, Gronke & Dijkstra 2016), another where there are only a few channels open for the LyC

photons to escape (ionized channels model, Zackrisson et al. 2013). In principle, the Ly α profile (shaped by the resonant interactions with the neutral hydrogen), could show evidence of these two different geometries (Rivera-Thorsen et al. 2017; Hutter et al. 2023, and references therein).

For a given galaxy, the number of ionizing (Lyman continuum, LyC) photons injected into the IGM per unit time can be expressed as

$$\dot{N}_{\text{ion}} = f_{\text{esc}}^{\text{LyC}} \xi_{\text{ion}} L_{\text{UV}}, \quad (1)$$

Where $f_{\text{esc}}^{\text{LyC}}$ (escape fraction of ionizing photons) represents the fraction of LyC photons that escape the galaxy with respect to the total amount produced by the young stellar population (in the case of GN-z8-LAE). In turn, ξ_{ion} (hydrogen ionizing photon production) can be understood as the number of hydrogen ionizing photons per unit of UV luminosity (e.g., Naidu et al. 2022; Lin et al. 2024), and is defined as:

$$\xi_{\text{ion}} = \frac{L_{\text{H}\beta}}{4.76 \times 10^{-13} (1 - f_{\text{esc}}) L_{\text{UV}}^{\text{int}}}. \quad (2)$$

From the above relations, it can be seen that $f_{\text{esc}}^{\text{LyC}}$ is a key parameter to determine \dot{N}_{ion} , and ξ_{ion} . However, the LyC emission can rarely be observed directly for $z > 4$ galaxies, as the mean-free path for LyC photons decreases exponentially with redshift (Inoue et al. 2014).

In the following sections, we will explore the possible contribution of galaxies like GN-z8-LAE to the reionization of the Universe and, particularly, the possibility of GN-z8-LAE efficiently injecting ionizing photons into the IGM.

4.1. Tracers of high LyC escape fraction

The literature has extensively explored the estimation of $f_{\text{esc}}^{\text{LyC}}$ using different tracers and techniques. Most studies rely on small samples of spectroscopically confirmed LyC leakers low- z analogs or simulations to predict whether a galaxy is a LyC leaker based on one or several of its observed properties.

Among the most relevant single-variable indicators for elevated LyC leakage, we find:

- Properties of the Ly α emission: Verhamme et al. (2017) found that LyC leakers preferentially have Ly α large rest-frame equivalent widths ($EW_0^{\text{Ly}\alpha} > 70 \text{ \AA}$) and escape fractions ($f_{\text{esc}}^{\text{Ly}\alpha} > 20\%$). More recent studies (e.g., Naidu et al. 2022; Izotov et al. 2021, using low- z analogs) suggest that leakers are characterized by a high $f_{\text{esc}}^{\text{Ly}\alpha}$, and more crucially, narrow Ly α profiles close to the systemic velocity (low values of $\Delta v_{\text{Ly}\alpha}$). This would indicate a highly transparent IGM. Chisholm et al.

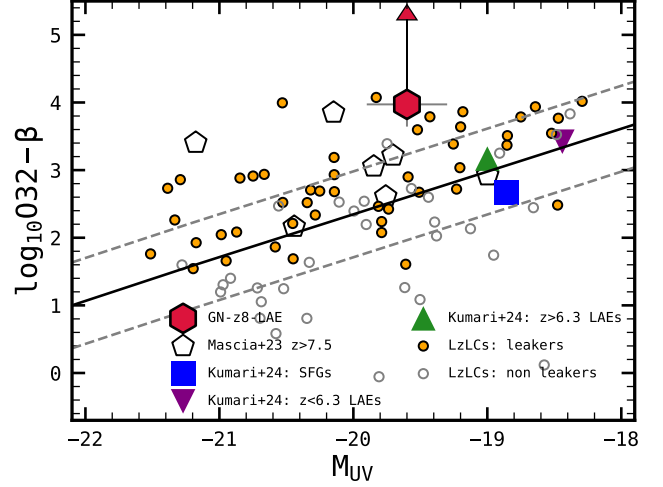


Figure 7. Diagnostic for classifying LyC leakers based on $\log_{10} \text{O32} - \beta$ vs M_{UV} as presented in Lin et al. (2024). The continuous line indicates the 50% probability of leaking LyC, while the discontinuous lines indicate the 25% and 75% values. GN-z8-LAE is shown as a red hexagon. We include the LzLCs divided into leakers and not leakers, the $z > 7.5$ simple compiled by Mascia et al. (2023a), and the average values for JADES SFGs, $z < 6.3$ LAEs and $z > 6.3$ LAEs reported in Kumari et al. (2024).

(2018) provides a estimation for $f_{\text{esc}}^{\text{LyC}}$ based on the dust-corrected $f_{\text{esc}}^{\text{Ly}\alpha}$.

- Dust content or β slope: Several works suggest that LyC leakers are characterized by blue β slopes and low dust content (Chisholm et al. 2022; Saldana-Lopez et al. 2022, for samples of low- z analogs). In particular, β was found to correlate with several parameters apart from dust content, such as $[\text{O III}] \lambda 5007 / [\text{O II}] \lambda \lambda 3726, 9$ (O32) ratio, but also metallicity, $EW_0^{\text{H}\beta}$, or stellar mass.
- Σ_{SFR} : Using the X-SHOOTER Lyman- α survey (XLS-z2, Matthee et al. 2021) sample, Naidu et al. (2020) argue that intense and compact star formation (high Σ_{SFR}) might create the necessary conditions (ionized channels) that allow for an efficient escape of LyC (and Ly α) photons (see Pucha et al. 2022; Trebitsch et al. 2017, $f_{\text{esc}}^{\text{LyC}}$ would be a feedback-regulated process).
- Elevated $\text{C IV} / \text{C III}]$ ratio and EW_0^{CIV} : The presence of strong nebular C IV (from its EW_0 or the $\text{C IV} / \text{C III}]$ ratio) has been identified as a proxy for enhanced $f_{\text{esc}}^{\text{LyC}}$ (e.g., Saxena et al. 2022; Schaerer et al. 2022, for samples of $z \sim 3 - 4$ SFGs and $z \sim 0.3 - 0.4$ LyC leakers).
- Elevated $[\text{O III}] \lambda \lambda 5007 / [\text{O II}] \lambda \lambda 3726, 3729$ (O32) ratio: Izotov et al. (2017); Flury et al. (2022) found

evidence of a correlation between the O32 line ratio for samples of low- z analogs (although this ratio depends strongly on the ionization parameter, Strom et al. 2018). More recent studies, however, seem to suggest O32 is not necessarily elevated for LyC leakers, or that the correlation is not so tight (Izotov et al. 2021).

- The presence of narrow Mg II $\lambda 2796,2803$ emission close to systemic velocity. (Chisholm et al. 2020; Xu et al. 2022)

Several recent works propose the use of multi-variable tracers as LyC leakage predictors. Interestingly, large departures from single-variable estimates have been reported (e.g., Fig. 6 of Jaskot et al. 2024a, where several multi-variate models are compared with predictions from Chisholm et al. 2022). Among these models, we highlight:

- Mascia et al. (2023a) studied a sample of high- z galaxies from the GLASS survey (Treu et al. 2022), and used a sample of low redshift analogs (from the from the Low-redshift Lyman Continuum Surve, LzLCs Flury et al. 2022) to calibrate an empirical relation between observed properties and $f_{\text{esc}}^{\text{LyC}}$. The relation takes the shape: $\log_{10}(f_{\text{esc}}^{\text{LyC}}) = A + B \log_{10}(\text{O32}) + C R_{\text{eff}}^{\text{UV}} + D \beta$, thus their model relies on three parameters (previously identified as individual tracers: $\log_{10}(\text{O32})$, β and $R_{\text{eff}}^{\text{UV}}$) to identify LyC leakers.
- Lin et al. (2024) used low- z analogs (LzLCs) to construct an indicator LyC leakage based on the β slope and O32 ratios, which is in good agreement with Mascia et al. (2023a) predictions.
- Jaskot et al. (2024b,a): use the LzLCs sample to build several predictors (using Cox proportional hazards models) with a broad range of observed parameters, then apply them to $z \sim 3$ and $z \sim 6$ samples. Models including dust attenuation ($E(B-V)$ or β) and the O32 ratio or morphological measurements ($R_{\text{eff}}^{\text{UV}}$, Σ_{SFR}) seem to be the best-performing to predict the $f_{\text{esc}}^{\text{LyC}}$ for the $z \sim 3$ sample.

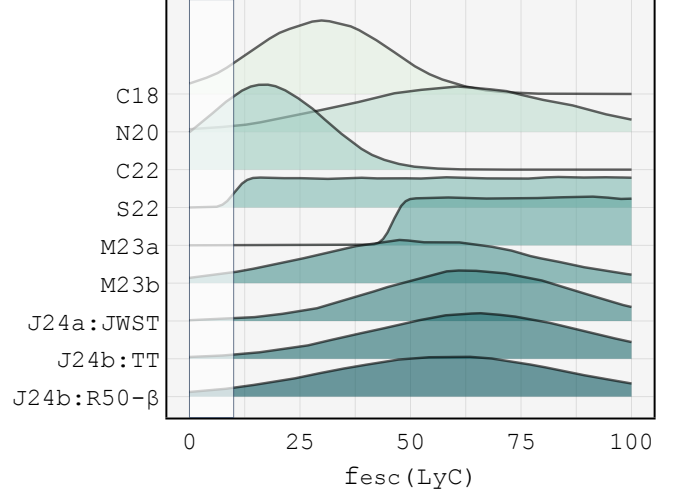


Figure 8. Visualization of the $f_{\text{esc}}^{\text{LyC}}$ for GN- $z8$ -LAE predicted by all indicators. We abbreviate the references as follows: C18 for Chisholm et al. (2018), N20 for Naidu et al. (2020), C22 for Chisholm et al. (2022), S22 Schaerer et al. (2022), M23a for Mascia et al. (2023a), M23b for Mascia et al. (2023b), J24a:JWST for Jaskot et al. (2024a): ‘Full JWST’, J24b:TT for Jaskot et al. (2024b): ‘Top Three’, J24b:R50- β for Jaskot et al. (2024b): ‘R50- β ’. We show in a white shade the area between $f_{\text{esc}}^{\text{LyC}} \sim 0-10$, as this is where typically non-leakers are located. The median values and corresponding uncertainties are reported in Table 6.

4.2. Estimating the LyC leakage for GN- $z8$ -LAE

We now apply the previously defined criteria to GN- $z8$ -LAE. Notably, all single variable from the above requirements are satisfied: a narrow Ly α which is close to ($\Delta v_{\text{Ly}\alpha} = 132 \pm 72$ km/s) and has residual emission at the systemic velocity, low dust content ($A_V < 0.1$) and blue β slope ($\beta = -2.48 \pm 0.23$), is compact and has an elevated value of $\Sigma_{\text{SFR}} = 88 \pm 32 M_{\odot}/\text{yr}/\text{kpc}^2$, presence of bright C IV and high $\text{C IV}/\text{C III}] = 3.3 \pm 1.4$ ratio, an elevated O32 > 30 (upper limit, as $[\text{O II}] \lambda\lambda 3727,9$ is not detected) and the presence of narrow Mg II close to the systemic velocity. We report the results for all indicators in Table 6.

By applying the relations described in Chisholm et al. (2018, 2022); Naidu et al. (2020); Schaerer et al. (2022), we recover an escape fraction compatible with the leakage of LyC photons.

We now explore the multi-variate indicators. The relation by Mascia et al. (2023a) leads to an elevated lower limit of $f_{\text{esc}}^{\text{LyC}}$, due to the upper limit in the O32 ratio. A similar answer is found when using Lin et al. (2024). This is shown in Fig. 7, where GN- $z8$ -LAE is located well above the discontinuous line of 75% probability of

Table 6. The estimated $f_{\text{esc}}^{\text{LyC}}$ of GN- z 8-LAE derived from different indirect indicators. In the case of Jaskot et al. (2024b,a) we report the $f_{\text{esc}}^{\text{LyC}}$ that satisfies $P(f_{\text{esc}}^{\text{LyC}}) < p$ for $p = (0.16, 0.50, 0.84)$.

Reference	Method	f_{esc}
Chisholm et al. (2022)	β	14 ± 14 %
Naidu et al. (2020)	Σ_{SFR}	60 ± 25 %
Chisholm et al. (2018)	$f_{\text{esc}}^{\text{Ly}\alpha}$	$\sim 25 - 40$ %
Schaerer et al. (2022)	C4C3 ^a	> 10 %
Mascia et al. (2023a)	O32, $\log_{10} R_{\text{eff}}^{\text{UV}}, \beta$	> 46 %
Mascia et al. (2023b)	$\text{EW}_0^{\text{H}\beta}, \log_{10} R_{\text{eff}}^{\text{UV}}, \beta$	53 ± 26 %
Jaskot et al. (2024b) ‘Top Three’	E(B-V), \log_{10} O32, $\log_{10} \Sigma_{\text{SFR}}$	40% – 60% – 100%
Jaskot et al. (2024b) ‘R50- β ’	$\beta, M_{\text{UV}}, M^*, \log_{10} R_{\text{eff}}^{\text{UV}}$	18% – 58% – 100%
Jaskot et al. (2024a) ‘Full JWST’	$M^*, M_{\text{UV}}, \log_{10} \text{EW}_0^{\text{H}\beta}, \text{E(B-V)}, 12 + \log_{10} \text{O/H},$ O32, $\log_{10} \Sigma_{\text{SFR}}, \beta$	44% – 65% – 100%
Lin et al. (2024)	$\beta, \text{O32}, M_{\text{UV}}$	leaker (P $\sim 99\%$)

^aC IV] $\lambda 1550/\text{C III] } \lambda 1909 > 0.75$

LyC leakage (this value is a lower limit, for the reasons above). Using their model, we recover a probability of $\sim 99\%$ of GN- z 8-LAE being a LyC leaker. Interestingly, the average values for LAEs/SFGs in JADES (Kumari et al. 2024) lie along/below the 50% probability line, respectively. This indicates that LyC leakers are uncommon in their sample, while GN- z 8-LAE shows several qualities in this direction.

By exploring several of the best-performing models from Jaskot et al. (2024b,a), namely: *Top Three*, *R50- β* and *Full JWST* models, we derive consistent multi-variable confirmation of the possible LyC nature of GN- z 8-LAE. Most observed properties, besides the ones concerning the Ly α emission, were used in this series of models. All models coincide in assigning a low probability to $f_{\text{esc}}^{\text{LyC}} < 20\%$, and predict mean values of $f_{\text{esc}}^{\text{LyC}} \sim 60\%$.

All this information is encoded in Fig. 8, which essentially displays the results of all indicators (Table 6). First of all, is clear that all indicators show evidence of an elevated LyC escape fraction ($f_{\text{esc}}^{\text{LyC}} > 10\%$). Interestingly, multi-variable indicators (shown downwards in the figure) tend to predict consistently higher $f_{\text{esc}}^{\text{LyC}}$ when compared to single-variable indicators. Similar effects have been also reported in the literature (e.g. Lin et al. 2024; Jaskot et al. 2024a).

Finally, we explored the predictions from the (minimal) model by Maji et al. (2022), calibrated using the Sphinx simulation post-processed using RASCAS (Michel-Dansac et al. 2020). However, in the case of GN- z 8-LAE, the model over-predicts the escape lumi-

nosity. This could be due to GN- z 8-LAE falling out of the SPHINX parameter space (e.g., SFR_{10} and $F_{\text{esc}}^{\text{Ly}\alpha}$).

If one message has to be conveyed from these analyses is that estimating $f_{\text{esc}}^{\text{LyC}}$ with indirect methods is not straightforward. Moreover, calibrations using $f_{\text{esc}}^{\text{Ly}\alpha}$ could be further affected by the complex physics ruling the properties of the Ly α line (Choustikov et al. 2024a). Nonetheless, all calibrations and observed properties agree on GN- z 8-LAE having a $f_{\text{esc}} \geq 20\%$, thus making it a strong Lyman continuum leaker candidate.

4.3. Hydrogen ionizing photon production efficiency

To make ξ_{ion} independent from the estimation of f_{esc} , which is indirect and uncertain for the vast majority of high- z galaxies, we introduce the quantity $\xi_{\text{ion}}^0 = \xi_{\text{ion}}(f_{\text{esc}}^{\text{LyC}} = 0)$ (Lin et al. 2024).

In the case of GN- z 8-LAE, we report $\log \xi_{\text{ion}}^0 = 25.78 \pm 0.15$ and $\xi_{\text{ion}} > 25.84$ assuming $f_{\text{esc}} \sim 14\%$ (the one recovered from the β slope). This value of ξ_{ion} is elevated with respect to the sample of HAEs studied by Rinaldi et al. (2023) ($\xi_{\text{ion}}^0 = 25.5 \pm 0.1$). In turn, this one was already enhanced relative to the typical ξ_{ion} reported in the literature at lower redshifts (e.g., Lam et al. 2019). Our high ξ_{ion}^0 value inferred for GN- z 8-LAE is however similar to that derived for the $z \sim 9$ source studied by Álvarez Márquez et al. (2024).

By following the discussion in Rinaldi et al. (2024a) and Atek et al. (2024), the average product $f_{\text{esc}} \times \xi_{\text{ion}}$ can be constrained from the progress of Cosmic Reionization. In the case of GN- z 8-LAE, this would impose an $f_{\text{esc}} \sim 5\%$ for $\xi_{\text{ion}}^0 = 25.78 \pm 0.15$, in agreement with what presented by Atek et al. (2024). In the light of our derivations of $f_{\text{esc}}^{\text{LyC}} \gg 5\%$, we argue that GN- z 8-LAE is

caught at the moment of being an efficient reionizer during the EoR.

5. SUMMARY AND DISCUSSION

We conducted a detailed analysis of the spectroscopic and photometric properties of GN- $z8$ -LAE, a prominent Ly α emitter at $z = 8.279$ selected from the JADES GOODS-N program. Some of these properties were studied before by Witstok et al. (2024a), with their derived parameter values being in broad agreement with ours in most cases. One notable exception is the UV β slope, though, for which we obtained a lower value ($\beta = -2.2 - -2.7$) than Witstok et al. (2024a), albeit consistent within the error bars. The reason for this departure might stem from the fact that we used the best-fit FUV continuum to determine β , while Witstok et al. (2024a) made use of the masked spectrum. Remarkably, GN- $z8$ -LAE is a low stellar-mass galaxy ($M^* \sim 10^{7.66} M_{\odot}$), contrary to the vast majority of Ly α emitters known at $z > 7$, which are typically significantly more luminous and massive.

Although GN- $z8$ -LAE is at too high a redshift to detect a significant amount of ionizing photons, we can conclude that this source is a robust candidate for a LyC leaker, namely an early reionizer. Indeed, our analysis of multiple indirect tracers univocally indicates that the f_{esc} of GN- $z8$ -LAE must be $> 10\%$, i.e. well above the average threshold needed for galaxies to drive the reionization process (Atek et al. 2024). Particularly, GN- $z8$ -LAE is a strong CIV] emitter, as expected for LyC leakers (Schaerer et al. 2022).

We also reported the detection of the NIII] λ 1749 – 1753 emission line complex in GN- $z8$ -LAE, which was not identified in previous studies of this source. Very recently, NIII] λ 1749 – 1753 was discovered in a handful of high- z galaxies (e.g., Marques-Chaves et al. 2024; Schaerer et al. 2024), but our source is the first reported case of simultaneous NIII] and Ly α emission at the EoR. As in Schaerer et al. (2024), our measured NIII] λ 1749 – 1753 flux implies a supra-solar N abundance, which is at odds with the sub-solar metallicity derived for our target.

The exact origin of the NIII] λ 1749 – 1753 is unclear, but Schaerer et al. (2024) suggested that there could be a link between this emission and extremely high values of Σ_{M^*} and Σ_{SFR} . This is confirmed for our source, which has $\Sigma_{M^*} \sim 355 M_{\odot}/\text{pc}^2$ and $\Sigma_{\text{SFR}} \sim 88 M_{\odot}/\text{yr}/\text{kpc}^2$ and, thus, is placed on the $\Sigma_{\text{SFR}}-\Sigma_{M^*}$ surface density relation derived by Morishita et al. (2024), along with other extreme density sources like previously found N-emitters. The NIII] λ 1749 – 1753 could also be associated

with the presence of Wolf-Rayet stars injecting N to the ISM (Rivera-Thorsen et al. 2024), but in this case we would also expect to see the permitted NIII] λ 4620, 4640 lines and broadened HeII λ 4686 emission, which we do not detect in GN- $z8$ -LAE.

In summary, GN- $z8$ -LAE is, to our knowledge, the most robust candidate found to date for a source being caught at the moment of reionizing its surrounding medium. *Which physical processes could lead to the properties observed in GN- $z8$ -LAE?* Based on magnetohydrodynamical galaxy simulations, Witten et al. (2024) concluded that prominent Ly α emission at the EoR could be explained via galaxy mergers inducing vigorous star formation. This remains to be investigated from the observational point of view. Further *JWST* observations should allow us to find more sources like GN- $z8$ -LAE in the early Universe and thoroughly study their properties, eventually leading to the unlock of the process of reionization.

6. ACKNOWLEDGMENTS

We thank Pratika Dayal for their useful discussions. RN and KIC acknowledge funding from the Dutch Research Council (NWO) through the award of the Vici Grant VI.C.212.036. E.I. and P.R. acknowledge funding from the Netherlands Research School for Astronomy (NOVA). This work is based on observations made with the NASA/ESA/CSA James Webb Space Telescope. The data were obtained from the Mikulski Archive for Space Telescopes at the Space Telescope Science Institute, which is operated by the Association of Universities for Research in Astronomy, Inc., under NASA contract NAS 5-03127 for *JWST*. These observations are associated with *JWST* programs GTO #1180, GO #1210, GO #1963 and GO #1895. The authors acknowledge the team led by coPIs D. Eisenstein and N. Luetzgendorf for developing their respective observing programs with a zero-exclusive-access period. Also based on observations made with the NASA/ESA Hubble Space Telescope obtained from the Space Telescope Science Institute, which is operated by the Association of Universities for Research in Astronomy, Inc., under NASA contract NAS 526555.

Software: AstroPy (Collaboration et al. 2022), BAGPIPES (Carnall et al. 2019a), dustmaps (Green 2018), Matplotlib (Hunter 2007), NumPy (Harris et al. 2020), Photutils (Bradley et al. 2022), PYTHON (van Rossum 1995), SciPy (Virtanen et al. 2020), TOPCAT (Taylor 2017), WebbPSF (Perrin et al. 2014).

Facilities: HST, JWST

REFERENCES

- Akerman, C. J., Carigi, L., Nissen, P. E., Pettini, M., & Asplund, M. 2004, *Astronomy and Astrophysics*, 414, 931, doi: [10.1051/0004-6361:20034188](https://doi.org/10.1051/0004-6361:20034188)
- Aller, L. H. 1984, *Astrophysics and Space Science Library*, doi: [10.1007/978-94-010-9639-3](https://doi.org/10.1007/978-94-010-9639-3)
- Asplund, M., Amarsi, A. M., & Grevesse, N. 2021, *Astronomy and Astrophysics*, 653, A141, doi: [10.1051/0004-6361/202140445](https://doi.org/10.1051/0004-6361/202140445)
- Atek, H., Labbé, I., Furtak, L. J., et al. 2024, *Nature*, 626, 975, doi: [10.1038/s41586-024-07043-6](https://doi.org/10.1038/s41586-024-07043-6)
- Berg, D. A., Erb, D. K., Henry, R. B. C., Skillman, E. D., & McQuinn, K. B. W. 2019, *The Astrophysical Journal*, 874, 93, doi: [10.3847/1538-4357/ab020a](https://doi.org/10.3847/1538-4357/ab020a)
- Berg, D. A., Skillman, E. D., Henry, R. B. C., Erb, D. K., & Carigi, L. 2016, *The Astrophysical Journal*, 827, 126, doi: [10.3847/0004-637X/827/2/126](https://doi.org/10.3847/0004-637X/827/2/126)
- Blaizot, J., Garel, T., Verhamme, A., et al. 2023, *Monthly Notices of the Royal Astronomical Society*, 523, 3749, doi: [10.1093/mnras/stad1523](https://doi.org/10.1093/mnras/stad1523)
- Bosman, S. E. I., Davies, F. B., Becker, G. D., et al. 2022, *Monthly Notices of the Royal Astronomical Society*, 514, 55, doi: [10.1093/mnras/stac1046](https://doi.org/10.1093/mnras/stac1046)
- Bouwens, R. J., Illingworth, G. D., Franx, M., et al. 2009, *The Astrophysical Journal*, 705, 936, doi: [10.1088/0004-637X/705/1/936](https://doi.org/10.1088/0004-637X/705/1/936)
- Bouwens, R. J., Oesch, P. A., Stefanon, M., et al. 2021, *The Astronomical Journal*, 162, 47, doi: [10.3847/1538-3881/abf83e](https://doi.org/10.3847/1538-3881/abf83e)
- Bradley, L., Sipőcz, B., Robitaille, T., et al. 2022, doi: [10.5281/ZENODO.7419741](https://doi.org/10.5281/ZENODO.7419741)
- Brammer, G. 2023, Zenodo, doi: [10.5281/zenodo.7299500](https://doi.org/10.5281/zenodo.7299500)
- Bruzual, G., & Charlot, S. 2003, *Monthly Notices of the Royal Astronomical Society*, 344, 1000, doi: [10.1046/j.1365-8711.2003.06897.x](https://doi.org/10.1046/j.1365-8711.2003.06897.x)
- Bunker, A. J., Saxena, A., Cameron, A. J., et al. 2023, *Astronomy and Astrophysics*, 677, A88, doi: [10.1051/0004-6361/202346159](https://doi.org/10.1051/0004-6361/202346159)
- Bunker, A. J., Cameron, A. J., Curtis-Lake, E., et al. 2024, *JADES NIRSpec Initial Data Release for the Hubble Ultra Deep Field: Redshifts and Line Fluxes of Distant Galaxies from the Deepest JWST Cycle 1 NIRSpec Multi-Object Spectroscopy*, arXiv, doi: [10.48550/arXiv.2306.02467](https://doi.org/10.48550/arXiv.2306.02467)
- Byler, N., Kewley, L. J., Rigby, J. R., et al. 2020, *The Astrophysical Journal*, 893, 1, doi: [10.3847/1538-4357/ab7ea9](https://doi.org/10.3847/1538-4357/ab7ea9)
- Calzetti, D., Kinney, A. L., & Storchi-Bergmann, T. 1994, *The Astrophysical Journal*, 429, 582, doi: [10.1086/174346](https://doi.org/10.1086/174346)
- Cameron, A. J., Saxena, A., Bunker, A. J., et al. 2023, *Astronomy & Astrophysics*, 677, A115, doi: [10.1051/0004-6361/202346107](https://doi.org/10.1051/0004-6361/202346107)
- Caputi, K. I., Deshmukh, S., Ashby, M. L. N., et al. 2017, *The Astrophysical Journal*, 849, 45, doi: [10.3847/1538-4357/aa901e](https://doi.org/10.3847/1538-4357/aa901e)
- Caputi, K. I., Caminha, G. B., Fujimoto, S., et al. 2021, *The Astrophysical Journal*, 908, 146, doi: [10.3847/1538-4357/abd4d0](https://doi.org/10.3847/1538-4357/abd4d0)
- Caputi, K. I., Rinaldi, P., Iani, E., et al. 2024, *The Astrophysical Journal*, 969, 159, doi: [10.3847/1538-4357/ad4eb2](https://doi.org/10.3847/1538-4357/ad4eb2)
- Carnall, A. C., Leja, J., Johnson, B. D., et al. 2019a, *The Astrophysical Journal*, 873, 44, doi: [10.3847/1538-4357/ab04a2](https://doi.org/10.3847/1538-4357/ab04a2)
- Carnall, A. C., McLure, R. J., Dunlop, J. S., et al. 2019b, *Monthly Notices of the Royal Astronomical Society*, 490, 417, doi: [10.1093/mnras/stz2544](https://doi.org/10.1093/mnras/stz2544)
- Carniani, S., Hainline, K., D'Eugenio, F., et al. 2024, *A shining cosmic dawn: spectroscopic confirmation of two luminous galaxies at $z \sim 14$* , doi: [10.48550/arXiv.2405.18485](https://doi.org/10.48550/arXiv.2405.18485)
- Caruana, J., Bunker, A. J., Wilkins, S. M., et al. 2014, *Monthly Notices of the Royal Astronomical Society*, 443, 2831, doi: [10.1093/mnras/stu1341](https://doi.org/10.1093/mnras/stu1341)
- Castellano, M., Napolitano, L., Fontana, A., et al. 2024, *JWST NIRSpec Spectroscopy of the Remarkable Bright Galaxy GHZ2/GLASS- z 12 at Redshift 12.34*, doi: [10.48550/arXiv.2403.10238](https://doi.org/10.48550/arXiv.2403.10238)
- Ceverino, D., Klessen, R. S., & Glover, S. C. O. 2018, *Monthly Notices of the Royal Astronomical Society*, 480, 4842, doi: [10.1093/mnras/sty2124](https://doi.org/10.1093/mnras/sty2124)
- Chisholm, J., Prochaska, J. X., Schaerer, D., Gazagnes, S., & Henry, A. 2020, *Monthly Notices of the Royal Astronomical Society*, 498, 2554, doi: [10.1093/mnras/staa2470](https://doi.org/10.1093/mnras/staa2470)
- Chisholm, J., Gazagnes, S., Schaerer, D., et al. 2018, *Astronomy & Astrophysics*, 616, A30, doi: [10.1051/0004-6361/201832758](https://doi.org/10.1051/0004-6361/201832758)
- Chisholm, J., Saldana-Lopez, A., Flury, S., et al. 2022, *Monthly Notices of the Royal Astronomical Society*, 517, 5104, doi: [10.1093/mnras/stac2874](https://doi.org/10.1093/mnras/stac2874)
- Choustikov, N., Stiskalek, R., Saxena, A., et al. 2024a, *Inferring the Ionizing Photon Contributions of High-Redshift Galaxies to Reionization with JWST NIRCам Photometry*, arXiv, <http://arxiv.org/abs/2405.09720>

- Choustikov, N., Katz, H., Saxena, A., et al. 2024b, *Monthly Notices of the Royal Astronomical Society*, 529, 3751, doi: [10.1093/mnras/stae776](https://doi.org/10.1093/mnras/stae776)
- Collaboration, T. A. T. A., Price-Whelan, A. M., Lim, P. L., et al. 2022, doi: [10.3847/1538-4357/ac7c74](https://doi.org/10.3847/1538-4357/ac7c74)
- Curti, M., Maiolino, R., Curtis-Lake, E., et al. 2024, *Astronomy & Astrophysics*, 684, A75, doi: [10.1051/0004-6361/202346698](https://doi.org/10.1051/0004-6361/202346698)
- Dayal, P., & Ferrara, A. 2018, *Physics Reports*, 780, 1, doi: [10.1016/j.physrep.2018.10.002](https://doi.org/10.1016/j.physrep.2018.10.002)
- D'Eugenio, F., Cameron, A. J., Scholtz, J., et al. 2024, *JADES Data Release 3 – NIRSpec/MSA spectroscopy for 4,000 galaxies in the GOODS fields*, doi: [10.48550/arXiv.2404.06531](https://doi.org/10.48550/arXiv.2404.06531)
- Donnan, C. T., McLeod, D. J., Dunlop, J. S., et al. 2023, *Monthly Notices of the Royal Astronomical Society*, 518, 6011, doi: [10.1093/mnras/stac3472](https://doi.org/10.1093/mnras/stac3472)
- Dopita, M. A., Fischera, J., Sutherland, R. S., et al. 2006, *The Astrophysical Journal Supplement Series*, 167, 177, doi: [10.1086/508261](https://doi.org/10.1086/508261)
- Eisenstein, D. J., Johnson, B. D., Robertson, B., et al. 2023a, *arXiv e-prints*, arXiv:2310.12340, doi: [10.48550/arXiv.2310.12340](https://doi.org/10.48550/arXiv.2310.12340)
- Eisenstein, D. J., Willott, C., Alberts, S., et al. 2023b, *Overview of the JWST Advanced Deep Extragalactic Survey (JADES)*, doi: [10.48550/arXiv.2306.02465](https://doi.org/10.48550/arXiv.2306.02465)
- Eldridge, J. J., Stanway, E. R., Xiao, L., et al. 2017, *Publications of the Astronomical Society of Australia*, 34, e058, doi: [10.1017/pasa.2017.51](https://doi.org/10.1017/pasa.2017.51)
- Emami, N., Siana, B., Weisz, D. R., et al. 2019, *The Astrophysical Journal*, 881, 71, doi: [10.3847/1538-4357/ab211a](https://doi.org/10.3847/1538-4357/ab211a)
- Endsley, R., Stark, D. P., Whitler, L., et al. 2023, *Monthly Notices of the Royal Astronomical Society*, 524, 2312, doi: [10.1093/mnras/stad1919](https://doi.org/10.1093/mnras/stad1919)
- Erb, D. K., Pettini, M., Shapley, A. E., et al. 2010, *The Astrophysical Journal*, 719, 1168, doi: [10.1088/0004-637X/719/2/1168](https://doi.org/10.1088/0004-637X/719/2/1168)
- Faisst, A. L., Capak, P. L., Emami, N., Tacchella, S., & Larson, K. L. 2019, *The Astrophysical Journal*, 884, 133, doi: [10.3847/1538-4357/ab425b](https://doi.org/10.3847/1538-4357/ab425b)
- Feltre, A., Charlot, S., & Gutkin, J. 2016, *Monthly Notices of the Royal Astronomical Society*, 456, 3354, doi: [10.1093/mnras/stv2794](https://doi.org/10.1093/mnras/stv2794)
- Ferland, G. J., Porter, R. L., van Hoof, P. A. M., et al. 2013, *Revista Mexicana de Astronomia y Astrofisica*, 49, 137, doi: [10.48550/arXiv.1302.4485](https://doi.org/10.48550/arXiv.1302.4485)
- Flury, S. R., Jaskot, A. E., Ferguson, H. C., et al. 2022, *The Astrophysical Journal*, 930, 126, doi: [10.3847/1538-4357/ac61e4](https://doi.org/10.3847/1538-4357/ac61e4)
- Fontana, A., Vanzella, E., Pentericci, L., et al. 2010, *The Astrophysical Journal*, 725, L205, doi: [10.1088/2041-8205/725/2/L205](https://doi.org/10.1088/2041-8205/725/2/L205)
- Gardner, J. P., Mather, J. C., Abbott, R., et al. 2023, *Publications of the Astronomical Society of the Pacific*, 135, 068001, doi: [10.1088/1538-3873/acd1b5](https://doi.org/10.1088/1538-3873/acd1b5)
- Garnett, D. R., Skillman, E. D., Dufour, R. J., et al. 1995, *The Astrophysical Journal*, 443, 64, doi: [10.1086/175503](https://doi.org/10.1086/175503)
- Geda, R., Crawford, S. M., Hunt, L., et al. 2022, *The Astronomical Journal*, 163, 202, doi: [10.3847/1538-3881/ac5908](https://doi.org/10.3847/1538-3881/ac5908)
- Gordon, K. D., Clayton, G. C., Misselt, K. A., Landolt, A. U., & Wolff, M. J. 2003, *The Astrophysical Journal*, 594, 279, doi: [10.1086/376774](https://doi.org/10.1086/376774)
- Green, G. M. 2018, *Journal of Open Source Software*, 3, 695, doi: [10.21105/joss.00695](https://doi.org/10.21105/joss.00695)
- Gronke, M., & Dijkstra, M. 2016, *The Astrophysical Journal*, 826, 14, doi: [10.3847/0004-637X/826/1/14](https://doi.org/10.3847/0004-637X/826/1/14)
- Gutkin, J., Charlot, S., & Bruzual, G. 2016, *Monthly Notices of the Royal Astronomical Society*, 462, 1757, doi: [10.1093/mnras/stw1716](https://doi.org/10.1093/mnras/stw1716)
- Hainline, K. N., Johnson, B. D., Robertson, B., et al. 2024, *The Astrophysical Journal*, 964, 71, doi: [10.3847/1538-4357/ad1ee4](https://doi.org/10.3847/1538-4357/ad1ee4)
- Hamann, F., Korista, K. T., Ferland, G. J., Warner, C., & Baldwin, J. 2002, *The Astrophysical Journal*, 564, 592, doi: [10.1086/324289](https://doi.org/10.1086/324289)
- Harikane, Y., Inoue, A. K., Ellis, R. S., et al. 2024, *JWST, ALMA, and Keck Spectroscopic Constraints on the UV Luminosity Functions at $z \sim 7-14$: Clumpiness and Compactness of the Brightest Galaxies in the Early Universe*, doi: [10.48550/arXiv.2406.18352](https://doi.org/10.48550/arXiv.2406.18352)
- Harris, C. R., Millman, K. J., Walt, S. J. v. d., et al. 2020, *Nature*, 585, 357, doi: [10.1038/s41586-020-2649-2](https://doi.org/10.1038/s41586-020-2649-2)
- Henry, R. B. C., Edmunds, M. G., & Köppen, J. 2000, *The Astrophysical Journal*, 541, 660, doi: [10.1086/309471](https://doi.org/10.1086/309471)
- Hirschmann, M., Charlot, S., Feltre, A., et al. 2019, *Monthly Notices of the Royal Astronomical Society*, 487, 333, doi: [10.1093/mnras/stz1256](https://doi.org/10.1093/mnras/stz1256)
- Humphrey, A. 2019, *Monthly Notices of the Royal Astronomical Society*, 486, 2102, doi: [10.1093/mnras/stz687](https://doi.org/10.1093/mnras/stz687)
- Hunter, J. D. 2007, *Computing in Science & Engineering*, 9, 90, doi: [10.1109/MCSE.2007.55](https://doi.org/10.1109/MCSE.2007.55)
- Hutter, A., Trebitsch, M., Dayal, P., et al. 2023, *Monthly Notices of the Royal Astronomical Society*, 524, 6124, doi: [10.1093/mnras/stad2230](https://doi.org/10.1093/mnras/stad2230)
- Iani, E., Caputi, K. I., Rinaldi, P., & Kokorev, V. I. 2022a, *The Astrophysical Journal Letters*, 940, L24, doi: [10.3847/2041-8213/aca014](https://doi.org/10.3847/2041-8213/aca014)

- Iani, E., Zanella, A., Vernet, J., et al. 2022b, doi: [10.1093/mnras/stac3198](https://doi.org/10.1093/mnras/stac3198)
- Iani, E., Caputi, K. I., Rinaldi, P., et al. 2024a, *The Astrophysical Journal*, 963, 97, doi: [10.3847/1538-4357/ad15f6](https://doi.org/10.3847/1538-4357/ad15f6)
- Iani, E., Rinaldi, P., Caputi, K. I., et al. 2024b, MIDIS: MIRI uncovers Virgil, an extended source at $z \sim 6.6$ with the photometric properties of Little Red Dots, doi: [10.48550/arXiv.2406.18207](https://doi.org/10.48550/arXiv.2406.18207)
- Inoue, A. K., Shimizu, I., Iwata, I., & Tanaka, M. 2014, *Monthly Notices of the Royal Astronomical Society*, 442, 1805, doi: [10.1093/mnras/stu936](https://doi.org/10.1093/mnras/stu936)
- Isobe, Y., Ouchi, M., Tominaga, N., et al. 2023, *The Astrophysical Journal*, 959, 100, doi: [10.3847/1538-4357/ad09be](https://doi.org/10.3847/1538-4357/ad09be)
- Izotov, Y. I., Chisholm, J., Worseck, G., et al. 2022, *Monthly Notices of the Royal Astronomical Society*, 515, 2864, doi: [10.1093/mnras/stac1899](https://doi.org/10.1093/mnras/stac1899)
- Izotov, Y. I., Stasińska, G., Meynet, G., Guseva, N. G., & Thuan, T. X. 2006, *Astronomy & Astrophysics*, 448, 955, doi: [10.1051/0004-6361:20053763](https://doi.org/10.1051/0004-6361:20053763)
- Izotov, Y. I., Thuan, T. X., & Guseva, N. G. 2017, *Monthly Notices of the Royal Astronomical Society*, 471, 548, doi: [10.1093/mnras/stx1629](https://doi.org/10.1093/mnras/stx1629)
- Izotov, Y. I., Worseck, G., Schaerer, D., et al. 2021, *Monthly Notices of the Royal Astronomical Society*, 503, 1734, doi: [10.1093/mnras/stab612](https://doi.org/10.1093/mnras/stab612)
- . 2018, *Monthly Notices of the Royal Astronomical Society*, 478, 4851, doi: [10.1093/mnras/sty1378](https://doi.org/10.1093/mnras/sty1378)
- Jaskot, A. E., & Ravindranath, S. 2016, *The Astrophysical Journal*, 833, 136, doi: [10.3847/1538-4357/833/2/136](https://doi.org/10.3847/1538-4357/833/2/136)
- Jaskot, A. E., Silveyra, A. C., Plantinga, A., et al. 2024a, *Multivariate Predictors of LyC Escape II: Predicting LyC Escape Fractions for High-Redshift Galaxies*, arXiv. <http://arxiv.org/abs/2406.10179>
- . 2024b, *Multivariate Predictors of LyC Escape I: A Survival Analysis of the Low-redshift Lyman Continuum Survey*, doi: [10.48550/arXiv.2406.10171](https://doi.org/10.48550/arXiv.2406.10171)
- Ji, X., Übler, H., Maiolino, R., et al. 2024, GA-NIFS: An extremely nitrogen-loud and chemically stratified galaxy at $z \sim 5.55$, doi: [10.48550/arXiv.2404.04148](https://doi.org/10.48550/arXiv.2404.04148)
- Juneau, S., Bournaud, F., Charlot, S., et al. 2014, *The Astrophysical Journal*, 788, 88, doi: [10.1088/0004-637X/788/1/88](https://doi.org/10.1088/0004-637X/788/1/88)
- Kennicutt, R. C. 1998, *Annual Review of Astronomy and Astrophysics*, 36, 189, doi: [10.1146/annurev.astro.36.1.189](https://doi.org/10.1146/annurev.astro.36.1.189)
- Kerutt, J., Oesch, P. A., Wisotzki, L., et al. 2024, *Astronomy & Astrophysics*, 684, A42, doi: [10.1051/0004-6361/202346656](https://doi.org/10.1051/0004-6361/202346656)
- Kokorev, V., Fujimoto, S., Labbe, I., et al. 2023, *The Astrophysical Journal*, 957, L7, doi: [10.3847/2041-8213/ad037a](https://doi.org/10.3847/2041-8213/ad037a)
- Kroupa, P. 2001, *Monthly Notices of the Royal Astronomical Society*, 322, 231, doi: [10.1046/j.1365-8711.2001.04022.x](https://doi.org/10.1046/j.1365-8711.2001.04022.x)
- Kulkarni, V. P., Cashman, F. H., Lopez, S., et al. 2019, *The Astrophysical Journal*, 886, 83, doi: [10.3847/1538-4357/ab4c2e](https://doi.org/10.3847/1538-4357/ab4c2e)
- Kumari, N., Smit, R., Witstok, J., et al. 2024, *JADES: Physical properties of Ly α and non-Ly α emitters at $z \sim 4.8$ -9.6*, arXiv, doi: [10.48550/arXiv.2406.11997](https://doi.org/10.48550/arXiv.2406.11997)
- Lam, D., Bouwens, R. J., Labbé, I., et al. 2019, *Astronomy & Astrophysics*, 627, A164, doi: [10.1051/0004-6361/201935227](https://doi.org/10.1051/0004-6361/201935227)
- Leitherer, C., Ferguson, H. C., Heckman, T. M., & Lowenthal, J. D. 1995, *The Astrophysical Journal*, 454, L19, doi: [10.1086/309760](https://doi.org/10.1086/309760)
- Leitherer, C., Schaerer, D., Goldader, J. D., et al. 1999, *The Astrophysical Journal Supplement Series*, 123, 3, doi: [10.1086/313233](https://doi.org/10.1086/313233)
- Lin, Y.-H., Scarlata, C., Williams, H., et al. 2024, *Monthly Notices of the Royal Astronomical Society*, 527, 4173, doi: [10.1093/mnras/stad3483](https://doi.org/10.1093/mnras/stad3483)
- Luridiana, V., Morisset, C., & Shaw, R. A. 2015, *Astronomy & Astrophysics*, 573, A42, doi: [10.1051/0004-6361/201323152](https://doi.org/10.1051/0004-6361/201323152)
- Maiolino, R., & Mannucci, F. 2019, *The Astronomy and Astrophysics Review*, 27, 3, doi: [10.1007/s00159-018-0112-2](https://doi.org/10.1007/s00159-018-0112-2)
- Maji, M., Verhamme, A., Rosdahl, J., et al. 2022, *Astronomy & Astrophysics*, 663, A66, doi: [10.1051/0004-6361/202142740](https://doi.org/10.1051/0004-6361/202142740)
- Marques-Chaves, R., Schaerer, D., Kuruvanthodi, A., et al. 2024, *Astronomy & Astrophysics*, 681, A30, doi: [10.1051/0004-6361/202347411](https://doi.org/10.1051/0004-6361/202347411)
- Mascia, S., Pentericci, L., Calabrò, A., et al. 2023a, *Astronomy & Astrophysics*, 672, A155, doi: [10.1051/0004-6361/202345866](https://doi.org/10.1051/0004-6361/202345866)
- . 2023b, *New insight on the nature of cosmic reionizers from the CEERS survey*, arXiv, doi: [10.48550/arXiv.2309.02219](https://doi.org/10.48550/arXiv.2309.02219)
- Matthee, J., Mackenzie, R., Simcoe, R. A., et al. 2023, *The Astrophysical Journal*, 950, 67, doi: [10.3847/1538-4357/acc846](https://doi.org/10.3847/1538-4357/acc846)
- Matthee, J., Sobral, D., Hayes, M., et al. 2021, *Monthly Notices of the Royal Astronomical Society*, 505, 1382, doi: [10.1093/mnras/stab1304](https://doi.org/10.1093/mnras/stab1304)

- Mazzolari, G., Übler, H., Maiolino, R., et al. 2024, New AGN diagnostic diagrams based on the [OIII] λ 4363 auroral line, arXiv, doi: [10.48550/arXiv.2404.10811](https://doi.org/10.48550/arXiv.2404.10811)
- McCarthy, P. J. 1993, *Annual Review of Astronomy and Astrophysics*, 31, 639, doi: [10.1146/annurev.aa.31.090193.003231](https://doi.org/10.1146/annurev.aa.31.090193.003231)
- Meurer, G. R., Heckman, T. M., & Calzetti, D. 1999, *The Astrophysical Journal*, 521, 64, doi: [10.1086/307523](https://doi.org/10.1086/307523)
- Meštrić, U., Vanzella, E., Zanella, A., et al. 2022, *Monthly Notices of the Royal Astronomical Society*, 516, 3532, doi: [10.1093/mnras/stac2309](https://doi.org/10.1093/mnras/stac2309)
- Michel-Dansac, L., Blaizot, J., Garel, T., et al. 2020, *Astronomy & Astrophysics*, 635, A154, doi: [10.1051/0004-6361/201834961](https://doi.org/10.1051/0004-6361/201834961)
- Mingozzi, M., James, B. L., Arellano-Córdova, K. Z., et al. 2022, *The Astrophysical Journal*, 939, 110, doi: [10.3847/1538-4357/ac952c](https://doi.org/10.3847/1538-4357/ac952c)
- Mingozzi, M., James, B. L., Berg, D. A., et al. 2024, *The Astrophysical Journal*, 962, 95, doi: [10.3847/1538-4357/ad1033](https://doi.org/10.3847/1538-4357/ad1033)
- Morishita, T., Stiavelli, M., Chary, R.-R., et al. 2024, *The Astrophysical Journal*, 963, 9, doi: [10.3847/1538-4357/ad1404](https://doi.org/10.3847/1538-4357/ad1404)
- Naidu, R. P., Tacchella, S., Mason, C. A., et al. 2020, *The Astrophysical Journal*, 892, 109, doi: [10.3847/1538-4357/ab7cc9](https://doi.org/10.3847/1538-4357/ab7cc9)
- Naidu, R. P., Matthee, J., Oesch, P. A., et al. 2022, *Monthly Notices of the Royal Astronomical Society*, 510, 4582, doi: [10.1093/mnras/stab3601](https://doi.org/10.1093/mnras/stab3601)
- Nakajima, K., & Ouchi, M. 2014, *Monthly Notices of the Royal Astronomical Society*, 442, 900, doi: [10.1093/mnras/stu902](https://doi.org/10.1093/mnras/stu902)
- Nakajima, K., Schaerer, D., Le Fèvre, O., et al. 2018, *Astronomy & Astrophysics*, 612, A94, doi: [10.1051/0004-6361/201731935](https://doi.org/10.1051/0004-6361/201731935)
- Navarro-Carrera, R., Rinaldi, P., Caputi, K. I., et al. 2023, *Constraints on the Faint End of the Galaxy Stellar Mass Function at $z \sim 4-8$ from Deep JWST Data*, arXiv, doi: [10.48550/arXiv.2305.16141](https://doi.org/10.48550/arXiv.2305.16141)
- Nicholls, D. C., Sutherland, R. S., Dopita, M. A., Kewley, L. J., & Groves, B. A. 2017, *Monthly Notices of the Royal Astronomical Society*, 466, 4403, doi: [10.1093/mnras/stw3235](https://doi.org/10.1093/mnras/stw3235)
- Oesch, P. A., Brammer, G., Naidu, R. P., et al. 2023, *The JWST FRESCO Survey: Legacy NIRCам/Grism Spectroscopy and Imaging in the two GOODS Fields*, arXiv. <http://arxiv.org/abs/2304.02026>
- Osterbrock, D. E., & Ferland, G. J. 2006, *Astrophysics of gaseous nebulae and active galactic nuclei*. <https://ui.adsabs.harvard.edu/abs/2006agna.book.....O>
- Ouchi, M., Ono, Y., & Shibuya, T. 2020, *Annual Review of Astronomy and Astrophysics*, 58, 617, doi: [10.1146/annurev-astro-032620-021859](https://doi.org/10.1146/annurev-astro-032620-021859)
- Pentericci, L., Fontana, A., Vanzella, E., et al. 2011, *The Astrophysical Journal*, 743, 132, doi: [10.1088/0004-637X/743/2/132](https://doi.org/10.1088/0004-637X/743/2/132)
- Perrin, M. D., Sivaramakrishnan, A., Lajoie, C.-P., et al. 2014, in *Space Telescopes and Instrumentation 2014: Optical, Infrared, and Millimeter Wave*, Vol. 9143 (SPIE), 1174–1184, doi: [10.1117/12.2056689](https://doi.org/10.1117/12.2056689)
- Proxauf, B., Öttl, S., & Kimeswenger, S. 2014, *Astronomy & Astrophysics*, 561, A10, doi: [10.1051/0004-6361/201322581](https://doi.org/10.1051/0004-6361/201322581)
- Pucha, R., Reddy, N. A., Dey, A., et al. 2022, *The Astronomical Journal*, 164, 159, doi: [10.3847/1538-3881/ac83a9](https://doi.org/10.3847/1538-3881/ac83a9)
- Pérez-Montero, E., & Amorín, R. 2017, *Monthly Notices of the Royal Astronomical Society*, 467, 1287, doi: [10.1093/mnras/stx186](https://doi.org/10.1093/mnras/stx186)
- Ramambason, L., Schaerer, D., Stasińska, G., et al. 2020, *Astronomy & Astrophysics*, 644, A21, doi: [10.1051/0004-6361/202038634](https://doi.org/10.1051/0004-6361/202038634)
- Ramos Almeida, C., Levenson, N. A., Alonso-Herrero, A., et al. 2011, *The Astrophysical Journal*, 731, 92, doi: [10.1088/0004-637X/731/2/92](https://doi.org/10.1088/0004-637X/731/2/92)
- Reddy, N. A., Topping, M. W., Sanders, R. L., Shapley, A. E., & Brammer, G. 2023a, *The Astrophysical Journal*, 952, 167, doi: [10.3847/1538-4357/acd754](https://doi.org/10.3847/1538-4357/acd754)
- Reddy, N. A., Sanders, R. L., Shapley, A. E., et al. 2023b, *The Astrophysical Journal*, 951, 56, doi: [10.3847/1538-4357/acd0b1](https://doi.org/10.3847/1538-4357/acd0b1)
- Rinaldi, P., Caputi, K. I., Costantin, L., et al. 2023, *The Astrophysical Journal*, 952, 143, doi: [10.3847/1538-4357/acdc27](https://doi.org/10.3847/1538-4357/acdc27)
- Rinaldi, P., Caputi, K. I., Iani, E., et al. 2024a, *The Astrophysical Journal*, 969, 12, doi: [10.3847/1538-4357/ad4147](https://doi.org/10.3847/1538-4357/ad4147)
- Rinaldi, P., Navarro-Carrera, R., Caputi, K. I., et al. 2024b, *The emergence of the Star Formation Main Sequence with redshift unfolded by JWST*, doi: [10.48550/arXiv.2406.13554](https://doi.org/10.48550/arXiv.2406.13554)
- Rivera-Thorsen, T. E., Dahle, H., Gronke, M., et al. 2017, *Astronomy & Astrophysics*, 608, L4, doi: [10.1051/0004-6361/201732173](https://doi.org/10.1051/0004-6361/201732173)
- Rivera-Thorsen, T. E., Chisholm, J., Welch, B., et al. 2024, *The Sunburst Arc with JWST: Detection of Wolf-Rayet stars injecting nitrogen into a low-metallicity, $Z=2.37$ proto-globular cluster leaking ionizing photons*, doi: [10.48550/arXiv.2404.08884](https://doi.org/10.48550/arXiv.2404.08884)

- Roberts-Borsani, G. W., Bouwens, R. J., Oesch, P. A., et al. 2016, *The Astrophysical Journal*, 823, 143, doi: [10.3847/0004-637X/823/2/143](https://doi.org/10.3847/0004-637X/823/2/143)
- Robertson, B. E., Ellis, R. S., Furlanetto, S. R., & Dunlop, J. S. 2015, *The Astrophysical Journal*, 802, L19, doi: [10.1088/2041-8205/802/2/L19](https://doi.org/10.1088/2041-8205/802/2/L19)
- Rosani, G., Caminha, G. B., Caputi, K. I., & Deshmukh, S. 2020, *Astronomy & Astrophysics*, 633, A159, doi: [10.1051/0004-6361/201935782](https://doi.org/10.1051/0004-6361/201935782)
- Rosdahl, J., Katz, H., Blaizot, J., et al. 2018, *Monthly Notices of the Royal Astronomical Society*, 479, 994, doi: [10.1093/mnras/sty1655](https://doi.org/10.1093/mnras/sty1655)
- Saldana-Lopez, A., Schaerer, D., Chisholm, J., et al. 2022, *Astronomy & Astrophysics*, 663, A59, doi: [10.1051/0004-6361/202141864](https://doi.org/10.1051/0004-6361/202141864)
- Sanders, R. L., Shapley, A. E., Topping, M. W., Reddy, N. A., & Brammer, G. B. 2024, *The Astrophysical Journal*, 962, 24, doi: [10.3847/1538-4357/ad15fc](https://doi.org/10.3847/1538-4357/ad15fc)
- Saxena, A., Cryer, E., Ellis, R. S., et al. 2022, *Monthly Notices of the Royal Astronomical Society*, 517, 1098, doi: [10.1093/mnras/stac2742](https://doi.org/10.1093/mnras/stac2742)
- Saxena, A., Robertson, B. E., Bunker, A. J., et al. 2023, *Astronomy and Astrophysics*, 678, A68, doi: [10.1051/0004-6361/202346245](https://doi.org/10.1051/0004-6361/202346245)
- Saxena, A., Bunker, A. J., Jones, G. C., et al. 2024, *Astronomy & Astrophysics*, 684, A84, doi: [10.1051/0004-6361/202347132](https://doi.org/10.1051/0004-6361/202347132)
- Schaerer, D., Marques-Chaves, R., Xiao, M., & Korber, D. 2024, *Discovery of a new N-emitter in the epoch of reionization*, arXiv. <http://arxiv.org/abs/2406.08408>
- Schaerer, D., Izotov, Y. I., Worseck, G., et al. 2022, *Astronomy & Astrophysics*, 658, L11, doi: [10.1051/0004-6361/202243149](https://doi.org/10.1051/0004-6361/202243149)
- Schenker, M. A., Ellis, R. S., Konidaris, N. P., & Stark, D. P. 2014, *The Astrophysical Journal*, 795, 20, doi: [10.1088/0004-637X/795/1/20](https://doi.org/10.1088/0004-637X/795/1/20)
- Senchyna, P., Plat, A., Stark, D. P., et al. 2024, *The Astrophysical Journal*, 966, 92, doi: [10.3847/1538-4357/ad235e](https://doi.org/10.3847/1538-4357/ad235e)
- Shibuya, T., Ouchi, M., Nakajima, K., et al. 2014, *The Astrophysical Journal*, 788, 74, doi: [10.1088/0004-637X/788/1/74](https://doi.org/10.1088/0004-637X/788/1/74)
- Sobral, D., & Matthee, J. 2019, *Astronomy & Astrophysics*, 623, A157, doi: [10.1051/0004-6361/201833075](https://doi.org/10.1051/0004-6361/201833075)
- Sparre, M., Hayward, C. C., Feldmann, R., et al. 2017, *Monthly Notices of the Royal Astronomical Society*, 466, 88, doi: [10.1093/mnras/stw3011](https://doi.org/10.1093/mnras/stw3011)
- Stanway, E. R., & Eldridge, J. J. 2018, *Monthly Notices of the Royal Astronomical Society*, 479, 75, doi: [10.1093/mnras/sty1353](https://doi.org/10.1093/mnras/sty1353)
- Stark, D. P., Ellis, R. S., Chiu, K., Ouchi, M., & Bunker, A. 2010, *Monthly Notices of the Royal Astronomical Society*, 408, 1628, doi: [10.1111/j.1365-2966.2010.17227.x](https://doi.org/10.1111/j.1365-2966.2010.17227.x)
- Stark, D. P., Richard, J., Siana, B., et al. 2014, *Monthly Notices of the Royal Astronomical Society*, 445, 3200, doi: [10.1093/mnras/stu1618](https://doi.org/10.1093/mnras/stu1618)
- Stark, D. P., Ellis, R. S., Charlot, S., et al. 2017, *Monthly Notices of the Royal Astronomical Society*, 464, 469, doi: [10.1093/mnras/stw2233](https://doi.org/10.1093/mnras/stw2233)
- Steidel, C. C., Pettini, M., & Adelberger, K. L. 2001, *The Astrophysical Journal*, 546, 665, doi: [10.1086/318323](https://doi.org/10.1086/318323)
- Storey, P. J., & Hummer, D. G. 1995, *Monthly Notices of the Royal Astronomical Society*, 272, 41, doi: [10.1093/mnras/272.1.41](https://doi.org/10.1093/mnras/272.1.41)
- Strom, A. L., Steidel, C. C., Rudie, G. C., Trainor, R. F., & Pettini, M. 2018, *The Astrophysical Journal*, 868, 117, doi: [10.3847/1538-4357/aae1a5](https://doi.org/10.3847/1538-4357/aae1a5)
- Sérsic, J. L. 1963, *Boletín de la Asociación Argentina de Astronomía La Plata Argentina*, 6, 41. <https://ui.adsabs.harvard.edu/abs/1963BAAA....6...41S>
- Taylor, M. 2017, arXiv e-prints, arXiv:1711.01885, doi: [10.48550/arXiv.1711.01885](https://doi.org/10.48550/arXiv.1711.01885)
- Topping, M. W., Stark, D. P., Senchyna, P., et al. 2024, *Monthly Notices of the Royal Astronomical Society*, 529, 3301, doi: [10.1093/mnras/stae682](https://doi.org/10.1093/mnras/stae682)
- Torralba-Torregrosa, A., Matthee, J., Naidu, R. P., et al. 2024, *Anatomy of an ionized bubble: NIRCам grism spectroscopy of the $z=6.6$ double-peaked Lyman- α emitter COLA1 and its environment*, doi: [10.48550/arXiv.2404.10040](https://doi.org/10.48550/arXiv.2404.10040)
- Trebitsch, M., Blaizot, J., Rosdahl, J., Devriendt, J., & Slyz, A. 2017, *Monthly Notices of the Royal Astronomical Society*, 470, 224, doi: [10.1093/mnras/stx1060](https://doi.org/10.1093/mnras/stx1060)
- Treu, T., Roberts-Borsani, G., Bradac, M., et al. 2022, *The Astrophysical Journal*, 935, 110, doi: [10.3847/1538-4357/ac8158](https://doi.org/10.3847/1538-4357/ac8158)
- van Rossum, G. 1995, *Python*
- Vanzella, E., Nonino, M., Cupani, G., et al. 2018, *Monthly Notices of the Royal Astronomical Society*, 476, L15, doi: [10.1093/mnrasl/sly023](https://doi.org/10.1093/mnrasl/sly023)
- Vanzella, E., Loiacono, F., Bergamini, P., et al. 2023, *Astronomy & Astrophysics*, 678, A173, doi: [10.1051/0004-6361/202346981](https://doi.org/10.1051/0004-6361/202346981)
- Verhamme, A., Orlitová, I., Schaerer, D., et al. 2017, *Astronomy & Astrophysics*, 597, A13, doi: [10.1051/0004-6361/201629264](https://doi.org/10.1051/0004-6361/201629264)
- Vila-Costas, M. B., & Edmunds, M. G. 1993, *Monthly Notices of the Royal Astronomical Society*, 265, 199, doi: [10.1093/mnras/265.1.199](https://doi.org/10.1093/mnras/265.1.199)

- Villar-Martín, M., Cerviño, M., & González Delgado, R. M. 2004, *Monthly Notices of the Royal Astronomical Society*, 355, 1132, doi: [10.1111/j.1365-2966.2004.08395.x](https://doi.org/10.1111/j.1365-2966.2004.08395.x)
- Virtanen, P., Gommers, R., Oliphant, T. E., et al. 2020, *Nature Methods*, 17, 261, doi: [10.1038/s41592-019-0686-2](https://doi.org/10.1038/s41592-019-0686-2)
- Watts, A. B., Catinella, B., Cortese, L., Power, C., & Ellison, S. L. 2021, *Monthly Notices of the Royal Astronomical Society*, 504, 1989, doi: [10.1093/mnras/stab1025](https://doi.org/10.1093/mnras/stab1025)
- Weisz, D. R., Johnson, B. D., Johnson, L. C., et al. 2012, *The Astrophysical Journal*, 744, 44, doi: [10.1088/0004-637X/744/1/44](https://doi.org/10.1088/0004-637X/744/1/44)
- Whitaker, K. E., Ashas, M., Illingworth, G., et al. 2019, *The Astrophysical Journal Supplement Series*, 244, 16, doi: [10.3847/1538-4365/ab3853](https://doi.org/10.3847/1538-4365/ab3853)
- Williams, H., Kelly, P. L., Chen, W., et al. 2023, *Science*, 380, 416, doi: [10.1126/science.adf5307](https://doi.org/10.1126/science.adf5307)
- Witstok, J., Maiolino, R., Smit, R., et al. 2024a, JADES: Primeval Lyman- α emitting galaxies reveal early sites of reionisation out to redshift $z \sim 9$, arXiv, doi: [10.48550/arXiv.2404.05724](https://doi.org/10.48550/arXiv.2404.05724)
- Witstok, J., Smit, R., Saxena, A., et al. 2024b, *Astronomy & Astrophysics*, 682, A40, doi: [10.1051/0004-6361/202347176](https://doi.org/10.1051/0004-6361/202347176)
- Witten, C., Laporte, N., Martin-Alvarez, S., et al. 2024, *Nature Astronomy*, 8, 384, doi: [10.1038/s41550-023-02179-3](https://doi.org/10.1038/s41550-023-02179-3)
- Witten, C. E. C., Laporte, N., & Katz, H. 2023, *The Astrophysical Journal*, 944, 61, doi: [10.3847/1538-4357/acac9d](https://doi.org/10.3847/1538-4357/acac9d)
- Xu, X., Henry, A., Heckman, T., et al. 2022, *The Astrophysical Journal*, 933, 202, doi: [10.3847/1538-4357/ac7225](https://doi.org/10.3847/1538-4357/ac7225)
- Xue, Y. Q., Luo, B., Brandt, W. N., et al. 2016, *The Astrophysical Journal Supplement Series*, 224, 15, doi: [10.3847/0067-0049/224/2/15](https://doi.org/10.3847/0067-0049/224/2/15)
- Yang, H., Wang, J., Zheng, Z.-Y., et al. 2014, *The Astrophysical Journal*, 784, 35, doi: [10.1088/0004-637X/784/1/35](https://doi.org/10.1088/0004-637X/784/1/35)
- Zackrisson, E., Inoue, A. K., & Jensen, H. 2013, *The Astrophysical Journal*, 777, 39, doi: [10.1088/0004-637X/777/1/39](https://doi.org/10.1088/0004-637X/777/1/39)
- Zitrin, A., Labbé, I., Belli, S., et al. 2015, *The Astrophysical Journal*, 810, L12, doi: [10.1088/2041-8205/810/1/L12](https://doi.org/10.1088/2041-8205/810/1/L12)
- Álvarez Márquez, J., Colina, L., Crespo Gómez, A., et al. 2024, *Astronomy and Astrophysics*, 686, A85, doi: [10.1051/0004-6361/202347946](https://doi.org/10.1051/0004-6361/202347946)